On boundary conditions and plastic strain-gradient discontinuity in lower-order gradient plasticity

Amit Acharya*, Huang Tang, Sunil Saigal

Civil and Environmental Engineering, Carnegie Mellon University, Pittsburgh, PA 15213, U.S.A

and

John L. Bassani

Mechanical Engineering and Applied Mechanics, University of Pennsylvania, Philadelphia, PA 19104, U.S.A.

Abstract

Through linearized analysis and computation, we show that lower-order gradient plasticity is compatible with boundary conditions, thus expanding its predictive capability. A physically motivated gradient modification of the conventional Voce hardening law is shown to lead to a convective stabilizing effect in 1-d, rate-independent plasticity. The partial differential equation is genuinely nonlinear and does not arise as a conservation law, thus making the task of inferring plausible boundary conditions a delicate matter. Implications of wave-type behavior in rate-independent plastic response (under conditions of static equilibrium) are analyzed with a discussion of an appropriate numerical algorithm. Example problems are solved numerically, showing the robustness and simplicity of physically-motivated lower-order gradient plasticity. The 3-d case and rate-dependent constitutive assumptions are also discussed.

1. Introduction

The question of deducing admissible boundary conditions (b.c.s) in the Simple Gradient Theory of Plasticity of Acharya and Bassani (1996, 2000) has been raised by the authors and in a recent paper by Volokh and Hutchinson (2002). As part of the analysis of a particular problem (simple shearing), the latter authors question the physical validity of the nature of b.c.s that they designate as applicable to the model. Furthermore, numerical calculations of Niordson and Hutchinson (2003) with the Simple Theory for a particular choice of hardening law demonstrate the phenomenon of 'vertex localization' with a trend towards localization of high strain in a narrow band, in small deformation hardening plasticity. Niordson and Hutchinson (2003) suggest that such a phenomenon is to be expected as a general feature of the Simple Theory due to the nature of its mathematical formulation and regardless of the specific choice of hardening description employed.

* Corresponding author: Tel. (412) 268 4566; Fax. (412) 268 7813; email: acharyaamit@cmu.edu

This paper presents an analysis of boundary conditions and a numerical algorithm related to the Simple Theory, in addition to a critical examination of the above findings. Our conclusions are as follows:

1. While the full nonlinear problem of evolution remains as analytically intractable as ever – this not being any different from the situation with other gradient theories of plasticity whether lower or higher-order - we are able to partially answer the question regarding b.c.s for the Simple Theory raised in Acharya and Bassani (2000) and Volokh and Hutchinson (2002), based on analysis of uniqueness of perturbations about arbitrary base states. Our conclusion is that the Simple Theory admits specifiable b.c.s of equal physical plausibility/incredibility as any other higher-order theory – in this we agree with Volokh and Hutchinson in principle, but feel that the absence of higher-order stress quantities with their complement of extra field equations in our theory is a definite advantage. The specifiable b.c.s are nonlinear, i.e. current state-dependent. When the current state (base state of the linearization) has certain spatial symmetry properties, e.g. symmetry about the mid-point of a 1-d domain, then b.c.s are admitted or not, on *both* ends of the domain, even though the (rate independent) evolution equation in question contains only first-order derivatives in both space and time. In other words, an equation that on first glance appears to admit only 'one-sided' b.c.s actually admits 'two-sided' ones or none, on an examination of details (an elementary example due to Friedrichs (1958) is given in the Appendix of this paper). This analysis does not support Volokh and Hutchinson's conjecture that the Simple Theory "does not appear to be in accord with basic physical requirements" (also see Fleck and Hutchinson (2001) in a slightly different context).

   As mentioned, our conclusions are based on uniqueness arguments for the linearized evolution equation. Uniqueness arguments based on 'energy' methods for linear partial differential equations (pde) typically do not preclude an overspecification of b.c.s. Overspecification, in a linear equation, leads to problems with existence of solutions in a suitable smoothness class. However, for a nonlinear equation (with state-dependent b.c.s) representing physics that is intended to stabilize the development of high gradients even such a problem need not arise, so that two-sided b.c.s may be imposed if the physics demands so. Our conclusions on this matter are tentative as the mathematics required to rigorously deduce the entire class of admissible b.c.s for the full nonlinear equation involved is a matter of nonlinear analysis that is unexplored at the current time, to the best of our knowledge.

However, we demonstrate plausibility of the idea through a computation based on an approximation scheme informed by mature concepts in the numerical analysis of first-order partial differential equations that produces a result which appears to be physically reasonable. Also, in the context of a slightly simplified version of the third-order, quasilinear spatial problem that arises in Volokh and Hutchinson (2002) upon using a separable solution ansatz, we demonstrate that four boundary conditions may be specified – while the equation dealt with here is slightly different from that in Volokh and Hutchinson (2002), we consider our analytical result as strong evidence to suggest their claim of only three specifiable conditions - and not more - as suspect.

2. We concur with Niordson and Hutchinson (2003) in predicting a localized band of plastic shear in hardening small-deformation plasticity for their choice of hardening function but with a different numerical scheme. Utilizing the same numerical scheme, we also demonstrate that such a feature is not a universal consequence of the theory. In particular, we adopt the hardening function proposed by Acharya and Beaudoin (2000) – shown to be successful in predicting the polycrystal size effect (Acharya and Beaudoin, 2000; Beaudoin *et al.*, 2000) and cleavage/orientation dependence in the fracture of ductile single crystals (Tang *et al.,* 2003a, b) within the Simple Gradient Theory framework for finite deformations (*a class of problems not addressed by any higher-order gradient theory*) – and show no localization of strain in narrow bands. In fact, we demonstrate a trend to absolute spatial homogeneity of initially inhomogeneous profiles, when allowed by boundary constraints.

   A loss of smoothness of solutions is observed – a smooth initial condition develops a kink at isolated points – a phenomenon termed as 'vertex localization' by Niordson and Hutchinson (2003). Such a kink is not observed to be accompanied by a localization of shear strain in a narrow band for all hardening models. While a large discontinuity in plastic strain - or, what is effectively the same, a large continuous variation of strain over a small region - in small deformation hardening plasticity would indeed be a cause for concern, we fail to see any adverse consequence of a discontinuity in the *gradient of plastic strain* in a continuous, small-magnitude, plastic strain profile.

3. In the context of the linearized, first-order pde for shearing of a rate-independent material defined within the Simple Theory we establish that, on certain segments of the boundary, additional boundary conditions should be specified; in the sequel we clearly define these segments. In addition, due to the wave-like nature of the full evolutionary problem (i.e., the solution to the pde in space and time), care must be

taken with the numerics. For example, the primarily centered difference scheme utilized by Niordson and Hutchinson (2003) succeeds in their calculations because the wave-like response implied by the hardening function they use, for their choice of material parameters, is very weak. We use an algorithm incorporating upwind methods coupled with Friedrichs' method that is shown to provide convergent solutions for various specifications of boundary conditions and hardening relations.

This paper is organized as follows: we set the stage in Section 2 by discussing the problem of simple shearing of an infinite slab addressed in Volokh and Hutchinson (2002). In Section 3, we consider the same physical problem as above for a general class of hardening laws and derive sufficient conditions for uniqueness of perturbations from an arbitrary base state. The linearized equation for perturbations also suggests reasons why qualitatively different solutions might be expected for different hardening functions. In Section 4, a numerical scheme is designed based on insights from the linearized analysis to solve the nonlinear problem. In Section 5 a suite of problems is solved to investigate the nature of solutions to our theory. The paper ends with concluding remarks in Section 6 where we motivate why the Simple Theory is indeed simpler than higher order theories in a practical sense. Given the uncertainty in physical interpretation and application of boundary conditions that arise in higher and lower-order gradient theories in general, an argument may be made that it is practically advantageous if the corresponding rate (incremental) problem for a gradient theory is closed without additional boundary conditions. This fact is of consequence in terms of utilizing computational algorithms of conventional plasticity for gradient plasticity applications. Of course, the main contribution of the present paper is to show that the lower-order theory can also accommodate additional b.c.s.

As a matter of terminology, whenever we refer to the term localization in this paper, we mean it in the classical sense of shear localization, with any reference to vertex localization being explicitly referred to as such.

2. Number of boundary conditions for equations whose coefficient of highest derivative can change sign

Motivated by the problem of simple shearing of an infinite slab considered by Volokh and Hutchinson (2002), our main goal in this section is to show that a third-order equation can admit four boundary conditions in appropriate circumstances.

Volokh and Hutchinson (2002) consider a special rate-independent hardening description of the form

$$\frac{\dot{\tau}}{\dot{\gamma}_p} = h\left(\gamma_p', \gamma_p\right) = \frac{n\gamma_0}{\tau_Y}\left(\frac{\left(\gamma_p/\gamma_0\right)^2}{\left(1+l^2\,\gamma_p'^2/\gamma_p\right)^m}\right)^{(n-1)/2n}, \tag{1}$$

where τ is the uniform shear stress, γ_p is the plastic strain field, $\gamma_p' = \partial\gamma_p/\partial x$ and the dot denotes a time-like derivative, and $n, \gamma_0, \tau_Y, m, l$ are material parameters. Capitalizing on the homogeneity of the hardening prescription, a class of separable solutions in 1-d space and time of the form

$$\begin{aligned} u_p(x,\nu) &= \alpha(\nu)\beta(x) \\ \gamma_p(x,\nu) &= u_p'(x,\nu) = \alpha(\nu)\beta'(x) \end{aligned} \tag{2}$$

is considered, where u_p is the 'plastic displacement' field that may be introduced in this 1-d setting and ν is a monotonically increasing parameter with time. The function β is shown to be governed by the equation

$$\beta''\left[(n-1)ml^2\beta'\beta''' + \left[1-(n-1)m\right]l^2\beta''^2 + \beta'^2\right] = 0, \tag{3}$$

when (1) and $(2)_2$ are substituted in the incremental equilibrium equations. At this juncture, the authors conclude that

> "due to the third order character of [(3)], one additional boundary condition can be imposed."

They impose one such condition at the left end of the domain and obtain numerical solutions to the quasilinear equation (3). In discussing such solutions, it is stated

> "One could have equally well imposed the one extra boundary condition at the right end, but not on both simultaneously."

Based on this notion and some reasonable notions of b.c.s on plastic strain arising from dislocation behavior which dictate the necessity or lack of specifiable b.c.s at *both* ends of the interval, they conclude that the lower-order theory predicates unphysical behavior.

The issue of necessary b.c.s for the problem (3) is quite complex. Given that it is possible for the coefficient of the highest derivative term in (3) to change sign over the domain, the issue of sufficient b.c.s gets quite interesting and complicated even in the setting of a linear equation (Friedrichs, 1958; see Appendix of this paper). It should also be noted that b.c.s for a given differential equation are generally not arrived at as necessary conditions for well-posedness even for linear equations, even though it would be nice to have such a procedure in hand when physical guidance on the matter is not available as in the case of physically-motivated gradient theories for bulk response. At best b.c.s arise as sufficient conditions for uniqueness and, as such,

a class of b.c.s for a given differential equation may not be ruled out without sufficient reason. Volokh and Hutchinson's (2002) main argument rests on the fact that a third order equation can admit only three boundary conditions and not more. We now proceed to construct solutions to a third-order equation that admits four boundary conditions and is a variant of (3).

We consider the equation

$$2A\beta''\beta''' + B\beta''^3 = 0 \tag{4}$$

on the interval $[-L, L]$ with $L > 0, A > 0, B < 0$ as constant parameters. The approximation to (3) involves treating β' as a positive constant and assuming $\beta' \ll 1$. Since $\beta' \sim \gamma$ the plastic strain, up to a multiplicative function of time only (Volokh and Hutchinson, 2002), both of these approximations may be considered reasonable. At any rate, considering (4) as an approximation of (3) is not essential to the point to be made here. In this section, we will often refer to β' as the plastic strain $\gamma = \gamma_p$.

To begin, it is clear that a solution of (4) with smooth plastic strain is $\beta'' \equiv 0$ with two boundary conditions to determine the function β. It can also be shown that $\beta'' \equiv 0$ is the unique solution of (4) for smooth β'' under the boundary conditions $\beta''(-L) = \beta''(L) = 0$. It bears emphasis that factoring out β'' in (4) and considering the class of solutions to the two factors set to zero does not encompass the entire class of solutions to (4). We now turn our attention to solutions of (4) with continuous but only piecewise-smooth plastic strain, i.e. β'' admits finite jump discontinuities. The required smoothness is appropriate for small deformation hardening plasticity. Clearly, (4) now needs an appropriate interpretation as a governing equation due to the presence of the terms β'', β'''. For this purpose, we pose (4) in variational form and infer the appropriate jump conditions at points of discontinuity.

Let φ be a differentiable function on $[-L, L]$ that vanishes in at least a small neighborhood of the boundary points of the domain. Then, we define a solution β to be a function that satisfies

$$\int_{-L}^{L} -\varphi' A\beta''^2 dx + \int_{-L}^{L} \varphi B\beta''^3 dx = 0 \quad \text{for all } \varphi \tag{5}$$

where each φ has the properties just mentioned. A β with an appropriately high degree of smoothness satisfying (5) also satisfies (4). However, (5) makes sense also for solutions β that have piece-wise continuous second derivatives (and, actually, for solutions with less smoothness).

For solutions in the smoothness class mentioned above, it can be shown – by choosing test functions φ that vanish everywhere in $[-L, L]$ except in arbitrarily small neighborhoods of a

point of discontinuity of β'' - that (5) implies the following jump condition at a point of discontinuity x^*:

$$\beta''^2_+\left(x^*\right)=\beta''^2_-\left(x^*\right), \tag{6}$$

where the left hand side of the above is the limit of the function involved as the point of discontinuity is approached from the right and the right hand side has a similar meaning as a limit approached from the left. For this problem the jump condition (6) implies a very strong restriction on the jump in the plastic strain gradient at any point: either the plastic strain gradient is continuous or the left-hand and right-hand slopes are exactly equal in magnitude and opposite in sign. Granted the existence of the separable solution and the validity of the assumption that the character of solutions to (4) resembles that of (3), we note here that the jump condition is a consequence of the physical requirements of force equilibrium, constitutive assumption, and a certain degree of smoothness of plastic strain.

The upshot of the weak formulation is that an admissible solution need satisfy (4) in regions where the plastic strain is sufficiently smooth and (6) where its slope is discontinuous.

It is an easy matter to determine two candidate functions for β'' that can be made to satisfy these conditions, each with a disposable parameter:

$$\begin{aligned}\beta''_- &= 2\left[\frac{B}{A}x+c_-\right]^{-1}\\ \beta''_+ &= -2\left[-\frac{B}{A}x+c_+\right]^{-1}.\end{aligned} \tag{7}$$

Our strategy will be to piece together a solution with the desired smoothness from the above two functions, using them appropriately in two parts of the domain. The two parameters c_+, c_- will be assigned through boundary conditions on β'' at *both* ends of the domain. The composite β'' function so determined can then be solved with two more boundary conditions to generate the solution β, thus utilizing four boundary conditions in all.

Let x^* be a point of discontinuity to be determined as part of the solution. Consider

$$\beta''(x)=\begin{cases}\beta''_-(x) & -L\le x\le x^*\\ \beta''_+(x) & x^*\le x\le L\end{cases} \tag{8}$$

with the b.c.s on the plastic strain gradient at the two ends given by

$$\begin{aligned}\beta''(-L)&=\beta''_-(-L)=S_-\\ \beta''(L)&=\beta''_+(L)=S_+.\end{aligned} \tag{9}$$

The constants c_-, c_+ take on the values

$$\begin{aligned} c_- &= \frac{B}{A}L + \frac{2}{S_-} \\ c_+ &= \frac{B}{A}L - \frac{2}{S_+}. \end{aligned} \tag{10}$$

Of the two possibilities implied by the jump condition (6), only one yields a meaningful constraint:

$$\beta_-''\left(x^*\right) = -\beta_+''\left(x^*\right) \quad \Rightarrow \quad x^* = -\frac{A}{B}\left[\frac{1}{S_-} + \frac{1}{S_+}\right]. \tag{11}$$

We observe that the point of discontinuity is controlled by the boundary conditions. In particular, if the boundary slopes are equal in magnitude and opposite in sign, then the discontinuity is always at the center of the domain, regardless of other parameter values. It appears to be possible to specify boundary conditions where the point of discontinuity specified by (11) may not be within the interval $\left[-L, L\right]$. The implications of this situation in terms of the (in)adequacy of the ansatz (8) is interesting, but we do not explore it here (a possibility is probably that two b.c.s are still admissible, but there are more points of discontinuity within the domain). Figures (1a,b) are qualitative sketches of the plastic strain and its gradient for the cases

$$\begin{aligned} -S_- &= S_+ = S > 0, \\ S_- &= -S_+ = S > 0, \end{aligned} \tag{12}$$

respectively. In this connection, we mention that the two constants c_+, c_- in (7) most probably can be determined by two boundary conditions on β' (plastic strain) with no further conditions on β'', while making sure that the point of discontinuity remains within the domain.

Before concluding this section we note that, in general, the specification of b.c.s at both ends (or none) is related to the singularity of the equation itself that can arise when *the coefficient of the highest-order derivative changes sign over the domain*. A closed-form example of such can be found in Friedrichs (1958) for a first-order, linear equation that admits b.c.s at both ends, where the square-integrable solution can be singular, discontinuous, continuous, or smooth depending upon parameter-values defining the problem (see the Appendix of this paper).

3. Boundary conditions from linearized analysis: the rate-independent material

With reference to Fig. 2 and within the framework of small strain theory, the equilibrium equation for the simple shearing of an infinite slab is $\tau_{12,1} = 0$, dictating that the shear stress be

homogeneous across the layer and given by applied traction $\tau_{12}(x_1,t)=\tau(t)$. We assume that the material is governed by a rate-independent constitutive law of the form

$$\dot{g}=h(\gamma_{,1},\gamma,g)\dot{\gamma}, \tag{13}$$

where g is the strength of the material, γ is the engineering plastic shear strain, $\gamma_{,1}=\partial\gamma/\partial x_1$, and h is a function specifying the hardening rate of the material. We define

$$T:=1/h. \tag{14}$$

Under conditions of continued plastic loading with monotonically increasing $\tau(t)$, the strength is also homogeneous and monotonically increasing, yielding the following evolutionary equation for the field γ:

$$\dot{\tau}=\dot{\tau}_{12}=\dot{g}=h\dot{\gamma} \quad \Rightarrow \quad \gamma_{,g}(x_1,g)=T(\gamma_{,1},\gamma,g). \tag{15}$$

For most physically realistic gradient hardening constitutive assumptions, (15) is expected to be genuinely nonlinear, i.e. it involves a nonlinear term in the gradient of plastic strain. For the case when $-T$ is convex in its first argument and does not contain a dependence on the second two arguments, mathematical analysis of global solutions for the initial value problem is available in the form of the Lax representation formula (Lax, 1973) and has been applied in Acharya *et al.* (1999). A method for generating local solutions to the scalar nonlinear first-order initial value problem also exists (John, 1982). Here, our interest is to infer some practical insight on the possible class of boundary conditions admitted by an equation of the general form (15) without any special convexity properties – in fact, a physically well-motivated hardening function that we will use shortly does not possess the required convexity property. Doing so for the general nonlinear case is hard. Moreover, the equation is not in divergence form so inferring natural b.c.s is not apparent. Even if this were possible, deciding on the parts of the boundary on which such a b.c. is applicable is not straightforward because of the first-order nature of the problem. Consequently, we focus on an analysis of perturbations from an arbitrary base state, expecting such analysis to provide some guidance on specifying boundary conditions in numerical approximation strategies whose discrete evolution in time is based on reasoning that applies to linear equations.

Let $\gamma(x_1,g)$ be a unique solution of (15), at point x_1 and load level $\tau=g$, arising from a set of specified initial and boundary data. Let the corresponding field at load level $\overline{g}=\overline{\tau}\leq\tau$ be $\gamma(x_1,\overline{g})=\overline{\gamma}(x_1)$. We define perturbations of the 'overbar' state in the natural way:

$$\begin{aligned}\gamma(x_1,g)-\overline{\gamma}(x_1) &=: \tilde{\gamma}(x_1,g)\\ g-\overline{g} &=: \tilde{g}.\end{aligned} \tag{16}$$

The governing equation for the perturbation $\tilde{\gamma}$ is now derived by substituting (16) in (15). As is usual, we assume that the individual perturbation quantities are 'small' as is the derivative of the plastic strain perturbation so that their products and higher-order multiples can be ignored. The following notation will also be employed: $\overline{T}$ will represent the function T evaluated at the base state $(\overline{\gamma}_{,1},\overline{\gamma},\overline{g})$ and $\overline{\partial_i T}, i=1,2,3$ will represent the derivative of the function T with respect to its three arguments in (15) from left to right, respectively, evaluated at the base state. The governing equation for the perturbation $\tilde{\gamma}$ is:

$$\tilde{\gamma}_{,g} = \overline{\partial_1 T}\ \tilde{\gamma}_{,1} + \overline{\partial_2 T}\ \tilde{\gamma} + \overline{\partial_3 T}\ \tilde{g} + \overline{T}\,. \tag{17}$$

The utility of (17) is that it exposes the velocity of the linearized wave of plastic strain as $V := -\overline{\partial_1 T}$. The minus sign is chosen to facilitate the physical interpretation of inflow, outflow and neutral boundary points to be defined below. With this convention, a wave moving in the positive x direction has positive velocity. It is also clear from (17) that different hardening relationships can lead to quite different growth behavior in solutions due to the presence of the last three source terms in (17). We remind the reader that in this particular problem the monotonic applied load/material strength plays the role of a time-like variable under conditions of static equilibrium. Therefore, these so-called plastic waves traveling at velocity V are not the usual waves that arise in solids due to inertial effects.

It is instructive, in the context of seeking insight into b.c.s for the actual nonlinear equation (15), to follow through with a uniqueness argument for solutions to (17). Physically, we would like our evolutionary specification to be such that (small but finite) perturbations out of an arbitrary base state are uniquely defined. To understand what specific conditions may be applied to achieve such uniqueness, consider the difference of two solutions to (17) denoted by χ which satisfies

$$\chi_{,g} = \overline{\partial_1 T}\ \chi_{,1} + \overline{\partial_2 T}\ \chi\,. \tag{18}$$

Multiplying (18) by χ and integrating by parts yields

$$\begin{aligned}&\frac{\mathrm{d}}{\mathrm{d}g}\int_0^H \chi^2 \mathrm{d}x_1 = \left(\overline{\partial_1 T}\ n\right)\chi^2\Big|_H + \left(\overline{\partial_1 T}\ n\right)\chi^2\Big|_0 + \int_0^H \left[2\overline{\partial_2 T} - (\partial_1 T)_{,1}\right]\chi^2 \mathrm{d}x_1,\\ &n(x_1 = H) = -n(x_1 = 0) = 1,\end{aligned} \tag{19}$$

where n in this 1-d setting is analogous to the outward unit normal.

Consider now the *boundary conditions* given by:

$$\left.\begin{array}{c}\tilde{\gamma}\\ or\\ \overline{\partial_1 T}\ \tilde{\gamma}\end{array}\right\} \text{ is specified at any boundary point } (x=0,H) \text{ where } \overline{\partial_1 T}\, n>0\,. \tag{20}$$

The boundary points on which conditions may be specified according to (20) form the inflow part of the boundary of the domain $(V\,n<0)$; boundary points where $V\,n>0$ form the outflow part of the boundary and a point where $V\,n=0$ forms a neutral point. Such inflow b.c.s, along with initial conditions, are physically natural as the set of specified data for transport processes, e.g., given the 1D-wave nature of (17), boundary data at $x=0$ or H propagates into the domain $(0<x<H)$ if $V\,n<0$.

If all perturbation solutions satisfy, at any boundary point, the same b.c.s out of the two possible ones in (20), then

$$\frac{d}{dg}\int_0^H \chi^2 dx_1 \le \int_0^H \left[2\overline{\partial_2 T}-(\partial_1 T)_{,1}\right]\chi^2 dx_1 \le \int_0^H \left|2\overline{\partial_2 T}-(\partial_1 T)_{,1}\right|\chi^2 dx_1\,, \tag{21}$$

where use has been made of the boundary condition to produce the crucial first inequality sign in (21). Let us assume that the term $\left|2\overline{\partial_2 T}-(\partial_1 T)_{,1}\right|$ is bounded in the domain, i.e. there exists, for each g, a positive constant $M(g)$ such that $\left|2\overline{\partial_2 T}\,(x_1,g)-\left(\overline{\partial_1 T}\right)_{,1}(x_1,g)\right|<M(g)$, and denoting $\int_0^H \chi^2(x_1,g)dx_1=\rho(g)$, (21) implies

$$\rho\left(g^*\right)\le\rho(\bar{g})+\int_{\bar{g}}^{g^*} M(g)\rho(g)dg\le\rho(\bar{g})\exp\left(\int_{\bar{g}}^{g^*} M(g)dg\right), \tag{22}$$

for $g^*\ge\bar{g}$ by the Gronwall Inequality. Since $\rho\left(g^*\right)$ is non-negative and $\rho(\bar{g})=0$ by definition (initial condition), (22) implies that the two perturbations forming the difference χ are identical almost everywhere.

A few things from the above analysis are to be especially noted:

1. First, since the inflow/outflow parts of the boundary depend upon the base state that may be spatially inhomogeneous, it is quite possible for the entire boundary (i.e., $x=0$ and $x=H$) to be inflow or outflow at some time, or for parts of it to be inflow and the rest outflow. Consequently, depending upon the base state, b.c.s may be imposed on the entire boundary, on none of it, or on parts of it.

2. Second, the uniqueness proof is not affected at all if a b.c. is specified on neutral points.
3. Third, the uniqueness proof for perturbations goes through even if b.c.s were to be specified on the outflow part along with the inflow part. Since the coefficients of the linearized equation (17) cannot respond to the evolving solution, such a specification could lead to the development of physically unexpected shocks in the solution of the linearized equations. However, in the nonlinear case this need not be true and physically plausible b.c. specification on the outflow boundary of the linearized equation should not be avoided.

To summarize, the above analysis reveals that the lower-order gradient theory is compatible with a minimal set of b.c.s, if not more, and identifies what variables may be specified.

Finally, we note that the above analysis generalizes naturally to the full 3-d case for a scalar dependent variable and, in the case of systems, if all (real) linear combinations of the linearized coefficient matrices, corresponding to the spatial partial derivatives of the perturbations, are diagonalizable (have a full set of real eigenvectors with real eigenvalues). As such, it might be of utility for inferring b.c.s for different constitutive theories leading to evolutionary systems (e.g. Acharya, 2003).

As a candidate hardening function that we work with subsequently, consider

$$h\left(\gamma_{,1}, g\right) = \frac{l\mu^2}{g - g_0}\alpha + \theta_0 \frac{g_s - g}{g_s - g_0} \ , \tag{23}$$

where $\alpha = \left|\gamma_{,1}\right|$ and $l, \mu, g_0, g_s, \theta_0$ are material constants. Note that in the absence of gradient hardening effects ($l = 0$), (23) can be integrated (in this rate-independent setting) to

$$g = g_s - \left(g_s - g_0\right)\exp\left(-\theta_0\left(\gamma - \gamma_*\right)/\left(g_s - g_0\right)\right), \ g\left(\gamma_*\right) = g_0 \tag{24}$$

Equation (23) maintains the form of the gradient enhanced Voce-law hardening model proposed in Acharya and Beaudoin (2000) and used to study the polycrystal size-effect, although the physical meaning of α as defined here is different from the forest dislocation density it replaces in the actual model, and this fact has an important implication with respect to hardening (or lack of it) due to a 'geometrically necessary' forest density in a purely 2-d, planar crystal plasticity setting (Beaudoin and Acharya, 2001). The corresponding linearized wave velocity is

$$V = -\overline{\partial_1 T} = h^{-2}\,\overline{\partial_1 h} = \frac{\operatorname{sgn}\left(\overline{\gamma}_{,1}\right)}{\overline{c}\left(\left|\overline{\gamma}_{,1}\right| + \dfrac{\overline{\theta}}{\overline{c}}\right)^2} \ , \tag{25}$$

where $\bar{c} = l\mu^2/(\bar{g} - g_0) > 0$, $\bar{\theta} = \theta_0 \dfrac{g_s - \bar{g}}{g_s - g_0} \geq 0$ and the symbol sgn represents the discontinuous function $sign(x)$, with $\text{sgn}(0)$ being undefined. Our analysis suggests that for a base state $\bar{\gamma}$ that is a convex function of x_1 with its minimum within the domain (see, e.g., Fig. 6), no b.c.s are required for uniqueness of perturbations. On the other hand, for a concave base state with maxima within the domain (see, e.g. Fig. 3), b.c.s can be applied to both ends to achieve uniqueness of perturbations.

The structure of (25) expressing the linearized wave velocity of plastic strain explains how a stabilizing effect arises for the considered model. A low plastic strain level is convected to regions of higher plastic strain. This is best understood by rephrasing the primary terms responsible for wave propagation in (17) in terms of γ instead of $\tilde{\gamma}$:

$$\gamma_{,g} = \overline{\partial_1 T}\ \gamma_{,1} + \overline{\partial_2 T}\ \tilde{\gamma} + \overline{\partial_3 T}\ \tilde{g} + \bar{T} - \overline{\partial_1 T}\ \bar{\gamma}_{,1}\,. \tag{26}$$

Moreover, for $\bar{g} \neq g_0$, $V = 0, \partial V/\partial l > 0$ for $l = 0$, i.e. for the conventional hardening there is no convective stabilization (of course) and the stabilization increases with increasing the magnitude of the internal material length scale. We also note that for fixed non-vanishing gradient at a point and $l \neq 0$, the wave speed vanishes at initial yield, $\bar{g} = g_0$ and only at this value. The velocity increases with increasing loading, at least initially, i.e. $\partial V/\partial \bar{g} > 0$ at initial yield, and at $\bar{g} = g_s$ the wave speed attains a finite non-zero value. Consequently, there is, at least, a range of initial loads beyond yield for which the stabilization effect increases. Also, in regions of low non-vanishing gradient the wave speed is generally higher thus providing a quicker stabilizing effect in such regions. If, on the other hand, the hardening function were such that the wave speed was to monotonically decrease with progress in loading and it were to be smaller in regions with smaller gradient, then this could lead to a localization type response if the conventional hardening and the current state were such as to provide the least hardening in the region of small gradients. We conjecture that this is perhaps one of the factors that leads to localization with the gradient hardening function of Bassani (2001), utilized in the work of Niordson and Hutchinson (2003).

4. Numerical algorithm for the 1-d rate-independent problem

The numerical scheme for solving the nonlinear equation (15) with the hardening function defined in (23) is built on the notion of the direction of linearized wave propagation of plastic strain defined in (25). We use upwind methods in which forward or backward difference methods at space levels are used to approximate the term $\gamma_{,1}$ - essentially, the continuum, linearized convection is followed in the numerical propagation of information. This is necessary,

as it is well-known that a centered-difference approximation to the simple first-order scalar wave equation with constant velocity is unconditionally unstable by Von-Neumann analysis (Strang, 1986). Indeed, we have confirmed such instability in our calculations for both choices of the hardening laws that we work with. Our numerical scheme utilizes upwinding with Friedrichs' scheme at nodes where the numerical gradient in plastic strain is zero (where there does not exist any special upwinding direction).

We use the following notation: $(\bullet)_n^k$ is used to represent the value of the $\bullet$ discrete field at the n^{th} node and k^{th} time-step; n_L and n_R, respectively, denote the node number corresponding to the left and right boundary, respectively. The algorithm for the upwind finite difference scheme is:

1. Choose the load increment Δg such that $\Delta g \le \omega \min(\left|\frac{\Delta x_1}{V(x_1)}\right|)$ to ensure stability, where $0 < \omega < 1$ is user defined.

2. $c^k = l\mu^2/(g^k - g_0)$, and if $g^k < g_s$, then $\theta^k = \theta_0 \frac{g_s - g^k}{g_s - g_0}$. If $g^k \ge g_s$, then $\theta^k = 0$.

3. Define $G_n^k = \frac{\gamma_{n+1}^k - \gamma_n^k}{2\Delta x_1}$ for interior nodes; $g^k = g_0 + k\Delta g$; $g^0 = g_0 + \Delta g$. G_n^k is a second-order accurate measure of the slope $\overline{\gamma}_{,1}$ that dictates the sign of V in (25).

4. Determine $\gamma_{,1}\Big|_n^k$: (*Note that this step is the crucial ingredient of the algorithm)*

   a) If $G_n^k < 0$, then $\gamma_{,1}\Big|_n^k = \frac{\gamma_{n+1}^k - \gamma_n^k}{\Delta x_1}$ (forward);

   b) If $G_n^k > 0$, then $\gamma_{,1}\Big|_n^k = \frac{\gamma_n^k - \gamma_{n-1}^k}{\Delta x_1}$ (backward);

   c) If $G_n^k = 0$, then $\gamma_{,1}\Big|_n^k = 0$;

5. Evaluate γ_n^{k+1} for interior nodes:

   a) If $G_n^k \ne 0$, then $\gamma_n^{k+1} = \gamma_n^k + \frac{\Delta g}{\left(c^k \left|\gamma_{,1}\Big|_n^k\right| + \theta^k\right)}$.

   b) If $G_n^k = 0$, then $\gamma_n^{k+1} = \frac{1}{2}\left(\gamma_{n-1}^k + \gamma_{n+1}^k\right) + \frac{\Delta g}{\theta^k}$ ($\theta^k \ne 0$) (Friedrichs' method).

6. Evaluate $G_{n_L}^k$ and $G_{n_R}^k$ at boundary point $x_1 = 0$ and $x_1 = H$, respectively:

a) $G_{n_L}^k = \dfrac{\gamma_{n_L+1}^k - \gamma_{n_L}^k}{\Delta x_1}$;

b) $G_{n_R}^k = \dfrac{\gamma_{n_R}^k - \gamma_{n_R-1}^k}{\Delta x_1}$;

7. Determine boundary conditions:

a) If $G_{n_L}^k \le 0$ (outflow), then $\gamma_{n_L}^{k+1} = \gamma_{n_L}^k + \dfrac{\Delta g}{\left(c^k \left|\gamma_{,1}\right|_{n_L}^k \right| + \theta^k\right)}$ (no boundary condition required);

b) If $G_{n_L}^k > 0$ (inflow), then $\gamma_{n_L}^{k+1} = \gamma_{n_L}^k$ (boundary condition 1) or $\gamma_{n_L}^{k+1} = \gamma_{n_L}^k + \dfrac{\Delta g}{\theta^k}$ (boundary condition 2);

Note: boundary condition 1 denotes that the current plastic strain is constrained to equal its previous value; boundary condition 2 requires that the plastic strains at the boundaries develop according to the conventional theory without gradient effects.

c) If $G_{n_R}^k \ge 0$ (outflow), then $\gamma_{n_R}^{k+1} = \gamma_{n_R}^k + \dfrac{\Delta g}{\left(c^k \left|\gamma_{,1}\right|_{n_R}^k \right| + \theta^k\right)}$ (no boundary condition required);

d) If $G_{n_R}^k < 0$ (inflow), then $\gamma_{n_R}^{k+1} = \gamma_{n_R}^k$ (boundary condition 1) or $\gamma_{n_R}^{k+1} = \gamma_{n_R}^k + \dfrac{\Delta g}{\theta^k}$ (boundary condition 2).

In the calculations conducted here, the height of the layer from $x_1 = 0$ to $x_1 = H$ is discretized using 161 nodes, unless otherwise specified.

5. Computational results for the 1-d rate-independent problem

With reference to the Voce hardening function (23), the length-scale parameter, l, takes the form

$$l = \frac{k_0 b \eta^2}{2}, \tag{27}$$

where η, a constant appearing in the well-established, empirical square-root of dislocation density dependence of the strength, takes a value of $1/3$, and the burgers vector magnitude $b = 0.2489nm$. The rest of the parameters are specified as follows: $g_s/g_0 = 1.8$, $\theta_0/g_0 = 3.9$, $\mu/g_0 = 800$. Here, g_s represents the saturation stress, g_0 the initial yield stress, μ the shear modulus, θ_0 the Stage II hardening rate $(\sim \mu/200)$, and k_0 is a fitting parameter. The

normalized length-scale parameter $k_0 b/H = 18\, l/H$ reflects the strength of the gradient term and is varied from a base value of 2×10^{-3} in the results that follow. The values above are suitable for a ductile material characterized by the conventional Voce-law hardening model. In addition, the load increment is held fixed at $\Delta g = 5\times10^{-8} g_0$ for most calculations. Most of the initial conditions chosen are identical to those in Niordson and Hutchinson (2003).

Before discussing results, we mention here that lower-order theories with gradient enhancement only in the hardening rate allow for a specification of initial strength independent of the plastic strain value. Niordson and Hutchinson (2003) show that choosing a uniform yield strength makes a tendency towards localization more pronounced. Moreover, the choice of the uniform initial distribution in 1-d calculations makes them simpler as an elastic-plastic boundary does not have to be tracked; all material points can load simultaneously, with the yield constraint satisfied at all times. Consequently, this is the choice of initial condition we adopt for the rate-independent results presented in this paper.

Non-uniform initial strain distributions

Figures 3 (a) and (b) depict the development of the normalized plastic strain with increasing load corresponding to $k_0 b/H = 2\times10^{-3}$ and $k_0 b/H = 2\times10^{-4}$, respectively. The initial distribution of plastic strain is upward parabolic in Figures 3 (a) and (b). This results in $\gamma_{,1} > 0$ at $x_1 = 0$, and $\gamma_{,1} < 0$ at $x_1 = H$. Consequently, boundary conditions are required on both boundaries. The conditions employed for the results in Fig. 3 correspond to requiring the boundary points evolve according to conventional gradient-independent plasticity (see boundary condition 2 of step 7 b in the numerical algorithm of Sec. 4), i.e. according to (23) with $l = 0$. The results clearly show that the plastic strain profiles tend to become homogeneous with increased load due to gradient effects. We note that the plastic strain distribution becomes uniform in Figure 3 (b) at a much higher load level than in Figure 3 (a) due to relatively weak gradient effects in the former (lower wave velocity as rationalized in Section 3), as measured by $k_0 b/H$. Gradients eventually disappear for both cases.

Next, the shear problem with the same initial imperfection as in Figure 3 (a) is evolved with the exception that no boundary conditions are imposed; the results are shown in Fig. 4. It is seen that the initially parabolic distribution of plastic strain becomes piecewise linear at large load level, implying uniform gradients across the layer, i.e. $\beta'' = \text{constant}$ with the jump at $x = x^* = H/2$ that satisfies (6). The profile of piecewise linearly distributed plastic strain is maintained with increased load. Even though boundary conditions are not imposed, convergence with respect to mesh refinement is observed for this particular case, as shown in Figure 5. We interpret this situation as one where the numerical scheme picks up a boundary condition that

ensures a physically reasonable solution (as in the 2D simulations of Bassani, et. al, 2001, and in 3D by Acharya and Beaudoin, 2000), in a sense, with the simplest discontinuity permitted.

Figures 6 (a) and (b) display the development of plastic strain profiles with increased load for the case of initially downward parabolic distribution of plastic strain. In these cases, we have $\gamma_{,1} < 0$ at $x_1 = 0$, and $\gamma_{,1} > 0$ at $x_1 = H$. As a result, boundary conditions are not required for the calculations. As shown in Figures 6 (a) and (b), the increase of plastic strain in the middle of the layer overwhelms the increase on the sides due to the distribution of gradients, which is lower in the middle and higher on the sides. The elimination of gradients spreads from the center, propagating through the entire layer[i]. Finally, the plastic strain becomes uniform across the layer. The process depends evidently on the gradient effects. It is seen that the process corresponding to Figure 6 (b) (smaller $k_0 b/H$) is much slower than that corresponding to Figure 6 (a).

The development of plastic strain profiles displayed in Figures 7 (a) and (b) corresponds to an initially bell-shaped distribution of plastic strain near $x = H/2$ and almost zero sufficiently far away from the center. This is a profile where each half of the initial distribution has concave and convex parts. In these cases, boundary conditions may or may not be imposed since $\gamma_{,1}$ is negligible at $x_1 = 0$ and $x_1 = H$. As shown in Figure 7, which is for the case of no boundary conditions applied, the development of plastic strain profiles is similar to those depicted in Figures 3 (for the concave part of the profile) and 6 (for the convex part of the profile). The plastic strain tends to be homogenous with increased load. The process is accelerated with higher strength of the gradient term.

Convergence of results is checked for the downward and upward parabolic initial conditions of plastic strain. Figure 8 (a) corresponding to the downward case compares the results for 161 nodes with $\Delta g = 5 \times 10^{-8} g_0$ and 1601 nodes with $\Delta g = 5 \times 10^{-9} g_0$, for a fixed value of total load and with no boundary conditions being required. Good convergence is obtained. Convergence is also shown in Figure 8 (b) for the upward parabolic initial distribution with boundary condition 2 (see step 7 b in the numerical algorithm of Sec. 4).

Our numerical scheme utilizes Friedrichs' scheme at nodes where the numerical gradient in plastic strain is zero. The reason for doing so is that there does not exist any special upwinding direction in this case and the centered-difference scheme is intrinsically unstable for first-order problems. While this choice of discretization does not make a difference when the actual distribution is homogeneous, at symmetric discontinuities in plastic strain-gradient, this factor

[i] David Owen has indicated to us that an analytical solution technique for scalar nonlinear evolutionary equations (John, 1982) assures the existence of local solutions to this problem, and that the gradient of plastic strain is the quantity that is propagated along characteristics.

plays a role. To illustrate the invariance of the results to this choice of discretization, we consider the following problem: identical solutions as before are expected when only the half width of the layer is modeled. Figure 9 shows the development of plastic strain for the case of the initially upward parabolic distribution with boundary condition 2 – the corresponding full-domain problem is shown in Figure 3 (a). In the calculation, the half width of the layer, from $x_1 = 0$ to $x_1 = H/2$, is discretized into 81 nodes. The point $x_1 = H/2$ has to be treated as boundary and a b.c. may or may not be required depending on the gradient at $x_1 = H/2$. In this case, no b.c.s are required at this point. To allow for a better comparison, the result in Figure 3 is superimposed on Figure 9, and identical solutions are obtained.

Zero strain boundary conditions

Next, we study the case of zero initial plastic strain with plastic strains constrained to be zero on the boundaries as the deformation evolves, which is similar to the problems considered by Shu *et al.* (2001) and Fleck and Hutchinson (2001). Indeed, this is an admissible boundary condition. Figures 10 (a, b, c, d) show that boundary layer phenomena may be predicted by the Simple Gradient theory when boundary conditions are accounted for. Figures 10 (a, b) show the development of plastic strain with the progress of loading for two choices of the gradient parameter. Figure 10 (c) shows the plastic strain profile, at fixed total applied displacement at the top of the layer, for a large range of values of the gradient parameter. This result shows the scaling of the 'boundary layer thickness' with the gradient parameter as well as a certain insensitivity of the maximum magnitude of plastic strain with respect to large variations in the gradient parameter, under fixed applied displacement. It is interesting to note the qualitative similarity of Figure 10(c) with the boundary layer result of Fleck and Hutchinson (2001, Fig. 1). Figure 10(d) shows the boundary layer effect at fixed applied load. Figure 10(e) are plots of the strength g, which in this problem corresponds to the shear stress, versus the average shear strain given in terms of the total displacement $u_2(H)$, showing that a stronger gradient effect in hardening leads to harder response.

A loss of smoothness in the gradient of plastic strain is observed at the center point for higher gradient strength (Figure 10 a, c, d). However, a trend towards localization of shear strain as described in Niordson and Hutchinson (2003) for a different hardening assumption does not emerge, regardless of the loss of smoothness of solutions. We attempt to put this comment in perspective by depicting, in Figure 11, the developing total displacement profiles corresponding to Figure 10 (a). As shown, the distribution of displacement across the layer is (of course) smooth without any sign of a typical profile corresponding to a shear band. The profile of plastic strain depicted in Figure 10 (a) also appears to be quite typical for cases corresponding to the imposition of zero boundary conditions on both boundaries, regardless of the initial distribution

of plastic strain. This is illustrated in Figure 12 where an initially symmetric piece-wise linear distribution of plastic strain with $k_0 b/H = 2\times10^{-3}$ is used. As shown, a similar profile of plastic strain as that in Figure 10 (a) develops. Figures 10(a, b) and 12 also provide evidence that the gradient in the hardening model does not lead to a sharper plastic strain profile with increasing deformation, where the qualifier 'sharp' refers to a higher rate of increase of magnitude of plastic strain gradient at the center than boundaries. Instead, the profiles seem to tend to a shape characterized by the gradient parameter strength, with the strain gradient near the boundaries increasing at a faster rate than in the interior.

Zero strain-increment boundary conditions

For a first order linear wave equation, an overspecification of b.c.s may lead to physically unacceptable solutions. However, it seems that this is not necessarily the case for the nonlinear equation considered here. This is illustrated in Figure 13 where an initially linear distribution of plastic strain is employed. According to the linearized analysis in Section 3, no boundary condition is required on the right boundary, initially. On the other hand, it may be argued that the layer could be placed in an environment that restricts any further increase in plastic strain at that boundary (Fleck and Hutchinson, 2001). Consequently, we hold the plastic strain on the right boundary fixed at its initial value for the entire course of the calculation, based on the rationalization provided in Sections 1 and 3 regarding b.c.s for the full nonlinear problem. As shown in Figure 13, a physically acceptable profile of plastic strain is seen to develop with a trend towards that of Figure 10 (a). The evolutionary equation responds to the applied b.c. at the right end so that soon after the initial instant the plastic strain profile adjusts so as to admit a b.c. at that end (according to linearized analysis).

Comparison with earlier work

The above results, and others to follow, corresponding to the 1-D rate independent case show that the gradient-enhanced Voce-law hardening imparts a stabilizing effect on plastic deformation. We check (Figure 14) that such a feature is not necessarily universal for all lower-order gradient models by repeating a calculation of Niordson and Hutchinson (2003) with our numerical scheme, utilizing the gradient hardening relationship given in Bassani (2001) and used in the calculations of Bassani *et al.* (2001). The hardening rate used for the calculation is given by (in the notation used here)

$$h(\gamma_{,1},\gamma) = \frac{\mu}{n}\left(\frac{\gamma}{\gamma_0}+1\right)^{\frac{1}{n}-1}\left[1+\frac{(l\gamma_{,1}/\gamma_0)^2}{1+c(\gamma/\gamma_0)^2}\right]^{1/2}, \tag{28}$$

where n is the strain hardening index, and c is an adjustable parameter. The parameter values for the calculation are $n=5$, $c=1$ and $l=2H$. The numerical upwinding considerations for this hardening assumption are identical to the other hardening law considered. In addition, the initial distribution of plastic strain is the same as that for Figure 4. Boundary conditions are not imposed in the calculations. As shown in Figure 14, the profile of plastic strain becomes sharper with increased load with a trend toward localization. This is perhaps attributable to the combined effects of a strong positive source term $\left(\overline{\partial_2 T}\right)\tilde{\gamma}$ in the linearized evolution (17) corresponding to (28) and the relatively low level of gradient stabilization due to reasons discussed at the end of Section 3. Therefore, we conclude that this simple hardening function (28) should be used with caution until its physical validity can be checked further. Nevertheless, we note that the type of behavior predicted in Fig. 14 may resemble the tendency for coarse slip (localized slip) in the early stage of deformation in ductile single crystals (Bassani, 1994).

An interesting question that arises in this context is the one of the effect of posing the plastic strain dependence of the hardening function in terms of strength, which for simple shearing must be uniform, and leaving the plastic strain gradient dependence of the hardening function as is. Clearly, similar distributions of plastic strain for the two cases are not to be expected in general. For a conventional stress-strain law of the form $\gamma=\gamma_0\left[\left(g/g_0\right)^n-1\right]$, the strength-based hardening relationship corresponding to (28) is

$$h(\gamma_{,1},g)=\frac{\mu}{n}\left(\frac{g}{g_0}\right)^{1-n}\left[1+\frac{(l\gamma_{,1}/\gamma_0)^2}{1+c((g/g_0)^n-1)^2}\right]^{1/2}; \tag{29}$$

Fig. 15 is a plot of developing plastic strain profiles for the same problem as in Fig. 14, with the difference that hardening is now characterized by (29). No tendency towards localization is seen, as opposed to Fig. 14.

We perform corresponding tests as above for the gradient-enhanced Voce law (23), simply to understand the effects of plastic strain and strain-gradient coupling in hardening. In the first case we employ the hardening function

$$h\left(\gamma_{,1},\gamma,g\right)=\frac{l\mu^2}{g-g_0}\alpha+\theta_0\exp\left(-\frac{\theta_0\gamma}{g_s-g_0}\right). \tag{30}$$

This amounts to writing only the conventional part of the hardening rate in terms of plastic strain according to (24) with $\gamma_*=0$, but the strength dependence of the gradient coefficient is left unaltered. The result corresponding to the problem description of Figure 4, but now with the hardening description (30), is shown in Fig. 16(a); the corresponding result to Fig. 10(b) is

shown in Fig. 16(b). No appreciable difference, between results for the strength or strain-based description for the conventional hardening, is observed in this case. These calculations have also been carried out to higher levels of stress without a qualitative change in our conclusions.

Next we employ a hardening description where the entire strength dependence of the gradient-enhanced Voce hardening is stated in terms of plastic strain, based on the stress-strain curve for homogeneous deformation (24) with $\gamma_* = 0$:

$$h(\gamma_{,1}, \gamma) = \frac{l\mu^2}{(g_s - g_0)\left(1 - \exp\left(-\theta_0 \gamma / g_s - g_0\right)\right)} \alpha + \theta_0 \exp\left(-\frac{\theta_0 \gamma}{g_s - g_0}\right). \tag{31}$$

Figure 16(c) shows the result for an upward parabolic initial plastic strain distribution. Indeed, at the boundary points the hardening is infinite and remains so through the course of the deformation and consequently there is no growth in plastic strain. The linearized wave-speed also vanishes at such points and these conditions are maintained through the deformation. However, at points in the interior the stabilizing effect of the gradient is evident (without it, there would be a sharpening of the profile). At a stress level $g/g_0 = 1.5$ the profile in Figure 14 has begun to sharpen whereas in Figure 16(c) the plastic strain-gradient is still higher near the boundaries than at the center. The reason for this qualitative difference may well be related to the arguments on variation of local wave-speed with increased loading given at the end of Section 3.

Based on the above results, it appears that an additive (as opposed to multiplicative) hardening relationship posed in terms of strength and strain-gradient is preferable in lower-order gradient plasticity, in particular if strain localization is to be suppressed. If a plastic strain based relationship has to be used, then multiplicative effects of plastic strain and strain gradient in hardening should be carefully considered.

6. Discussion

Two issues related to lower-order gradient plasticity have been dealt with in this paper: admissibility of b.c.s and vertex localization. We emphasize that these two issues are not related in the sense of the formation of vertices being necessary for the admissibility of additional b.c.s, as can be understood from the remarks in the last paragraph of Section 2 related to the example in the Appendix, as well as from the curve for $k_0 = 0.202$ in Figure 10(c).

Shear and Vertex Localization

Although basic characteristics of local constitutive equations can be studied from uniform stress and strain states, gradient-type equations require some degree of non-uniformity. Perhaps the most elementary example of the latter is 1-d shear, a problem that has received considerable attention in the context of plastic boundary layers. In that case the shear stress is uniform while

the shear strain can be non-uniform. Nevertheless, particularly in the context of a lower-order theory, it is important to note that such a state is a rather special example of a broader class of problems where the strain gradient is non-trivially constrained by differential equations of equilibrium and compatibility.

The recent attention to size-dependent phenomena in metal plasticity has been focused primarily on a class of materials for which 'smaller is harder.' To describe such behavior, gradient-type models have been constructed around the assumption that the yield strength and/or hardening rate increase with increasing plastic strain gradients, while the conventional hardening rate (i.e., if gradients are absent) tends to decrease with increasing strain. In a so-called lower-order theory, i.e. one in which higher-order stresses are absent, those characteristics lead to trends whereby regions of high strain and low strain gradient tend to be relatively soft compared to regions of lower strain and higher gradients. In simple shear, one might then expect that a region of maximum shear strain and zero strain gradient will tend to localize strain as Niordson and Hutchinson (2003) have suggested. *That, in fact, is not necessarily the case*. We demonstrate hardening functions that are easily generalized to a class of hardening assumptions, that lead to a stabilizing effect in such a scenario.

The 'source' term $\overline{T}$ in the linearized equation (26) accounts for the relative softening discussed above in a region where the strain is maximum and gradient is zero (we note in passing that this is also the only term that appears on the right hand side of the conventional incremental problem). Therefore, in the absence of any nontrivial effects of the differential constraints of equilibrium and compatibility in simple shearing, the only possible counter-balance to localization are the other terms entering the linearized evolution equation (26) for γ. Of these, the most significant is the convection term $\overline{\partial_1 T}\,\gamma_{,1}$. For the hardening function (23), this term tends to locally translate the initial profile (for the linearized equation) *in the direction of increasing plastic strain*, as can be seen from considering solutions of the form $\gamma_0\left(x_1 - Vg\right)$ to $\gamma_{,g} = \overline{\partial_1 T}\,\gamma_{,1} = -V\gamma_{,1}$, thus resulting in a decrease in plastic strain almost everywhere with the progress of loading. Consequently, whether the plastic strain profile localizes or not depends very much upon this convective stabilization counteracting the destabilizing effect of the term $\overline{T}$.

Based on the above understanding, we conclude that hardening constitutive equations that ensure linearized wave propagation in the direction of the plastic strain gradient without significant diminution with increase of loading ensure non-localizing behavior. Strength and plastic strain-gradient dependent hardening constitutive assumptions seem to be better suited for such a purpose than plastic strain and strain-gradient dependent hypotheses. Additionally, an additive contribution to conventional local hardening from the gradient term is to be preferred.

As shown in our calculations (Fig. 10 (c)), plastic strain gradient discontinuities or vertices may or may not form depending on the magnitude of the gradient-hardening effect. It seems to us that the experimental identification of the existence of vertices, as opposed to shear localization, from measured displacements would necessarily be fraught with uncertainty as can be observed even in the idealized case represented by the total displacement plot of Figure 11. It is our belief that the existence of a vertex in the absence of shear localization is physically immaterial.

Boundary Conditions

On a somewhat practical level, it has to be recognized that general b.c. specification dictated by gradient theory, both lower and higher-order, is not readily decided based solely upon physical considerations. Quantities like microforces (Gurtin, 2002) or higher-order stress vectors (Fleck and Hutchinson, 2001), plastic strain, slip, and strength do not lend themselves to manipulation by agents external to the body in which these fields are evolving. In light of the above, it can be argued that a b.c. decided by a computational algorithm is as good (or as bad) as one decided by the user, provided calculations are shown to be independent of discretization.

Previous works on lower-order theory (Acharya and Bassani (1996, 2000)) have consistently emphasized the non-necessity of additional b.c.s in defining the *incremental problem* (Hill, 1958), with due reservation expressed in the case of the actual evolutionary problem (Acharya and Bassani, 2000). The advantage of lower-order gradient plasticity lies in the fact that because of the incremental problem being closed without additional b.c.s beyond those required for the conventional theory, it appears that algorithms that can provide physically reasonable results independent of discretization and without the imposition of b.c.s for the evolutionary problem – or, in other words, stable algorithms that 'pick up' *a* b.c. when required - can be designed, and this feature has been utilized in producing stable numerical computations at finite strains with lower-order theory. Afore-cited examples include Acharya and Beaudoin (2000), and Bassani *et al*. (2001). Higher-order theories, on the other hand, require specified additional b.c.s for the solution of even the incremental problem.

In this context, it is perhaps important to clarify the Volokh-Hutchinson (2002) example of non-uniqueness of solutions in lower-order theory, apparently in the incremental problem. We note that an unambiguous (unique) specification of the current state of the entire body is an essential ingredient for defining the incremental boundary value problem (Hill, 1958). On the other hand Volokh and Hutchinson's (2002) analysis provides an equation for the determination of the spatial variation of the current plastic strain field corresponding to a separable solution ansatz. Putting these observations together, the most definite conclusion that we are able to draw

from the Volokh-Hutchinson analysis is that if the specified current plastic strain field is not of the form

$$\text{constant} \times \beta' \tag{32}$$

where β is a solution of (3), then the incremental boundary value problem does not admit a solution of the form (32) for the plastic strain rate out of the current state. Assuming loading everywhere and the current hardening rate as positive everywhere, it may also be further concluded that if the current plastic strain field is of the form (32), then the plastic strain rate out of the current state is of the same form as (32) with a different, but identifiable, constant, and, more importantly, that it is uniquely defined by the *unambiguously specified* current plastic strain field and the b.c.s that are part of the definition of the conventional incremental problem, without the need for any additional b.c.s. It bears emphasis that conditions for uniquely determining the current state are not, strictly speaking, relevant to understanding the issue of uniqueness of solutions to the incremental problem – in this sense, the issue of uniqueness of solutions to (3) arising in the Volokh-Hutchinson analysis, while relevant to understanding the evolutionary problem of lower-order theory, is slightly different from the issue of uniqueness of solutions to the incremental boundary value problem. We emphasize here that the incremental problem for lower-order gradient theory (gradient in tangent moduli) is closed with exactly the same requirements – including b.c.s - as for posing the incremental problem for conventional gradient-independent plasticity (Acharya and Shawki, 1995).

This paper is a first step in the direction of understanding the nature of the evolutionary problem of lower-order theory. A corresponding understanding for higher-order theory of the Fleck-Hutchinson type is lacking at the current time as can be seen from the considerations in the following paragraph. For the higher-order theory of Gurtin (2002), the evolution equation for the plastic distortion $\boldsymbol{F}^p$ is explicit in the time derivative while being nonlinear in the second spatial derivative of $\boldsymbol{F}^p$. The proposed micro-free and microclamped boundary conditions appear to provide Neumann or Dirichlet type b.c.s in this case, but no mathematical analysis is available as to their adequacy for well-posedness and the admissibility of other possible b.c.s.

We consider the higher-order governing equations for simple shearing of an infinite layer according to Fleck-Hutchinson (2001) theory:

$$\begin{aligned} 3S_{,t} &= -l^2\left[h\left(E_p\right)\gamma_{p,xt}\right]_{,x} + h\left(E_p\right)\gamma_{p,t} \\ \left(E_{p,t}\right)^2 &= \frac{1}{3}\left(\gamma_{p,t}\right)^2 + \frac{1}{3}l_*^2\left(\gamma_{p,tx}\right)^2 \end{aligned} \tag{33}$$

where E_p is the effective plastic strain, S is the applied shear traction, and comma denotes partial differentiation. It is an obvious implication of the evolutionary problem (33), i.e. governing equations for γ_p, E_p as functions of space and *time*, that in any finite (as opposed to infinitesimal) interval of time, the fields γ_p, E_p at the end of the time interval cannot be determined by the solution of the rate or incremental problem; the latter concerns solving the boundary value problem for $E_{p,t}$ and $\gamma_{p,t}$ as functions of space arising from evaluating (33) at the beginning of the time interval and assuming that the fields γ_p, E_p are known. Moreover,

(33) does not have the standard structure of evolutionary pde in the sense that the time derivatives of the basic fields at a typical spatial point cannot be expressed as functions of the values of the fields and spatial derivatives of the fields at that point; instead, the time derivatives in (33) may only be abstractly classified as being *functionals* of the fields γ_p, E_p - assuming the existence of suitable kernels (that may not be easy to determine due to the dependence of h on E_p), (33) may be classified as a system of evolutionary, nonlinear integro-partial differential equations or, as written down in (33), as evolutionary pde with implicit time derivatives. While this may not be an issue in stating the nonlinear evolutionary problem of Fleck-Hutchinson theory, from the point of view of mathematical analysis the problem is non-standard, unlike that of lower-order theory. The conditions that render the full problem of evolution closed have not been spelled out in Fleck-Hutchinson theory, with sufficient conditions that render solutions of the incremental problem unique being specified. That conditions different from those applicable to the incremental problem may also be applicable to higher-order theory at second-order in perturbations and for the full evolutionary problem cannot be ruled out.

The issue of adequate b.c.s (and well-posedness) in any gradient theory is, of course, a difficult question because of the nonlinearities inherent in plastic response and due to the coupling between internal variables and actual total deformation. Our comments are simply meant to emphasize the fact that the adequacy of b.c.s for the actual nonlinear evolutionary problem is an open problem for all gradient plasticity theories, whether lower or higher-order. An understanding of the matter could well affect the selection of computational schemes and the resulting approximate solutions for *both* lower and higher-order gradient theories.

Rate-dependence and 3-d problems in lower-order theory

As is well-known, systems of first-order, evolutionary partial differential equations present significantly different challenges than their scalar counterpart. For rate-dependent, gradient-enhanced Voce law type constitutive assumptions (Acharya and Beaudoin, 2000), it can be shown that the linearized system of evolution equations for the plastic distortion are weakly hyperbolic in the sense that all (real) linear combinations of the linearized coefficient matrices, corresponding to the spatial partial derivatives of the perturbations, have real eigenvalues (in

fact, all zero) but not an associated full set of eigenvectors[ii]. By theory for first-order systems this entails linear growth with wavenumber and makes the linear system sensitive to lower-order perturbations to the principal part, the latter most often resulting in exponential growth in large wavenumbers. However, remarkably, such growth occurs in the strength variable for the constitutive assumption under consideration, and this has the effect of cutting off plasticity and such 'linearized' growth (physically, the material is stronger in its response to small wave-length perturbations), thereby rendering a stabilizing effect which is observed in calculations we have performed. Of course, making the last argument sound and hence ensuring that the physical expectation, and numerical experience, is realized without exception for an appropriate class of initial data would require strict nonlinear analysis of first-order systems that will be the scope of future work.

On the matter of inferring admissible boundary conditions in this case, the principal part of the linearized system is not symmetric and hence using 'energy method' type arguments to infer b.c.s is not possible. However, if it may be assumed that the plastic distortion evolution is continuously dependent on initial data, an assumption that may not be unreasonable due to the argument related to linearized growth in strength mentioned above, the linearized equations may be formally Laplace transformed and a b.c.(s) on strength inferred, even for the 3-d, crystal plasticity case. Such an exercise has been conducted and, interestingly, yields an interface condition involving all five grain boundary parameters, among other things, when applied to grain boundaries.

The plausible property of continuous dependence of solutions with respect to initial data for the system arising from the rate-dependent gradient enhanced Voce law would also be shared by the constitutive class of power-law rate-dependency with gradient only in the hardening modulus. For the rate-independent, multidimensional case – system as opposed to scalar – characterized by equations (essentially) of the form

$$\dot{\boldsymbol{P}} = \boldsymbol{\Pi}\left(\dot{\gamma}\right) \quad ; \quad \dot{\gamma} = \frac{\dot{\tau}}{h\left(\nabla \boldsymbol{P}, \boldsymbol{P}, \gamma \text{ or } s\right)} \quad ; \quad \dot{s} = H\left(s\right)\dot{\gamma} \tag{34}$$

($\boldsymbol{\Pi}$ gives the direction of plastic flow), or other gradient models of plasticity where the gradient is introduced directly in the strength, i.e. rate-dependent models of the form

$$\dot{\boldsymbol{P}} = \boldsymbol{\Pi}\left(\dot{\gamma}\right) \quad ; \quad \dot{s} = H\left(s\right)\dot{\gamma} \quad ; \quad \dot{\gamma} = \left(\frac{\tau}{Y\left(\nabla \boldsymbol{P}, \boldsymbol{P}, s\right)}\right)^{\frac{1}{m}}, \tag{35}$$

[ii] We note that issues of hyperbolicity discussed here are not related to the ellipticity, or lack of it, for the incremental equilibrium equations.

the gradient of plastic distortion appears explicitly in the expression for the rate of plastic distortion, and symmetry in the linearization is not guaranteed. In such situations, some assessment of growth of plastic strain dictated by the model is advisable. Of course, our comment is not meant to imply that such a feature necessarily implies any sort of instability in the actual *nonlinear* problem. In fact, even though there does not appear to be a lot in common in the mathematical appearance of the rate-dependent gradient-enhanced Voce law system and systems of the type (34) or (35), the physical ideas behind all of these models are quite similar and so it is natural to expect similarity in the actual mathematical details and solutions corresponding to these systems. Higher-order evolutionary systems like (33) could also benefit from similar study of growth behavior of solutions; again, an understanding could very well affect computational schemes as well as approximate solutions of higher-order theory.

7. Acknowledgment

We wish to thank J. W. Hutchinson for provoking our latest round of thought on the subject of this paper by making available copies of his work with K. Y. Volokh and C. F. Niordson before publication. We thank D. Owen for his interest and comments on this work, and Shlomo Ta'asan for a discussion of first-order systems. Financial support from NSF-Sandia Life Cycle Engineering Initiative and from NSF CMS 99-00131 are gratefully acknowledged.

8. References

Acharya, A. and Shawki, T. G. (1995) Thermodynamic restrictions on constitutive equations for second-deformation-gradient inelastic behavior, *Journal of the Mechanics and Physics of Solids,* 11, 1751-1772.

Acharya, A. and Bassani, J. L. (1996) On non-local flow theories that preserve the classical structure of incremental boundary value problems, in IUTAM symposium on *Micromechanics of Plasticity and Damage of Multiphase Materials*, Ed. A. Pineau and A. Zaoui, 3-9, Kluwer Academic Publishers.

Acharya, A., Cherukuri, H. P. and Govindarajan, R. M. (1999) A new proposal in gradient plasticity: theory and application in 1-d quasi-statics and dynamics, *Mechanics of Cohesive-Frictional Materials*, 4, 153-170.

Acharya, A. and Bassani, J. L. (2000) Lattice incompatibility and a gradient theory of crystal plasticity, *Journal of the Mechanics and Physics of Solids*, 48, 1565-1595.

Acharya, A. and Beaudoin, A. J. (2000) Grain-size effect in FCC viscoplastic polycrystals at moderate strains, *Journal of the Mechanics and Physics of Solids,* 48, 2213-2230.

Acharya, A. (2003) Driving forces and boundary conditions in continuum dislocation mechanics, *Proceedings of the Royal Society, London, A*, 459, 1343-1363.

Bassani, J. L., "Plastic Flow of Crystals," *Advances in Applied Mechanics*, **30**, pp. 191-258, 1994.

Bassani, J. L. (2001) Incompatibility and a simple gradient theory of plasticity, *Journal of the Mechanics and Physics of Solids,* 49, 1983-1996.

Bassani, J. L., Needleman, A., and Van der Geissen, E. (2001) Size effects in composites: A comparison of nonlocal plasticity and discrete dislocation predictions, *International Journal of Solids and Structures,* 38, 833-853.

Beaudoin, A. J., Acharya, A., Chen, S. R., Korzekwa, D. A. and Stout, M. G. (2000) Consideration of grain-size effect and kinetics in the plastic deformation of metal polycrystals, *Acta Materialia*, 48, 3409-3423.

Beaudoin, A. J. and Acharya, A. (2001) A model for rate-dependent flow of metal polycrystals based on the slip plane lattice incompatibility, *Materials Science and Engineering*, A-309-310, 411-415.

Fleck, N. A. and Hutchinson, J. W. (2001) A reformulation of strain gradient plasticity, *Journal of the Mechanics and Physics of Solids,* 49, 2245-2271.

Friedrichs, K. O. (1958) Symmetric positive linear differential equations, *Communications on Pure and Applied Mathematics,* XI, 333-418.

Gurtin, M. E. (2002) A gradient theory of single crystal viscoplasticity that accounts for geometrically necessary dislocations, *Journal of the Mechanics and Physics of Solids,* 50, 5-32.

Hill, R. (1958) A general theory of uniqueness and stability in elastic-plastic solids, *Journal of the Mechanics and Physics of Solids,* 6, 236-249.

John, F. (1982) Partial Differential Equations, Applied Mathematical Sciences, 1, Springer-Verlag.

Lax, P. D. (1973) Hyperbolic systems of conservation laws and the mathematical theory of shock waves, CBMS series, SIAM.

Niordson, C. F. and Hutchinson, J. W. (2003) On lower order strain gradient plasticity theories, To be published in *European Journal of Mechanics, A/Solids*.

Peirce, D., Asaro, R. J. and Needleman, A. (1983) Material rate dependence and localized deformation in crystalline solids, *Acta Metallurgica,* 31, 1087-1119.

Shu, J. Y., Fleck, N. A., Van der Giessen, E. and Needleman, A. (2001) Boundary layers in constrained plastic flow: comparison of nonlocal and discrete dislocation plasticity, *Journal of the Mechanics and Physics of Solids,* 49, 1361-1395.

Strang, G. (1986) Introduction to Applied Mathematics, Wellesley-Cambridge Press.

Tang, H., Choi, Y. S., Acharya, A. and Saigal, S. (2003 a) Effects of lattice incompatibility-induced-hardening on the fracture behavior of ductile single crystals. *Submitted.*

Tang, H., Acharya, A. and Saigal, S. (2003 b) Directional dependence of crack growth along the interface of a bicrystal with symmetric tilt Boundary in the presence of gradient effects. *Preprint.*

Volokh, K. Yu. and Hutchinson, J. W. (2002) Are lower order gradient theories of plasticity really lower order? To be published in *Journal of Applied Mechanics.*

Appendix

Friedrichs (1958) demonstrates, even in the case of ODEs, that a differential equation with a singularity associated with the coefficient of the highest derivative changing sign can admit more (or fewer) b.c.s than one would anticipate from the order of the equation. In the Introduction, he considers the simple, first-order, Euler-type ODE:

$$2\alpha' x\frac{\mathrm{d}u}{\mathrm{d}x}+\gamma u=f(x),\qquad x_-\le x\le x_+,\qquad x_-<0,x_+>0. \tag{A1}$$

with the requirement that $u(x)$ be square integrable in the domain and $\gamma>\alpha'$. In the case of $\alpha'<0$, a unique square-integrable solution is obtained in terms of two b.c.s that determine the two constants c_+, c_- in

$$u(x)=u_0(x)+c_+\,u_+(x)+c_-\,u_-(x) \tag{A2}$$

where,

$$u_0(x)=\int_{x_0}^{x} f(x')\left|\frac{x'}{x}\right|^{\gamma/2\alpha}\frac{\mathrm{d}x'}{2\alpha' x'}, \tag{A3}$$

$$u_\pm(x)=\begin{cases}(\pm x)^{-\gamma/2\alpha'} & \text{for } \pm x>0\\ 0 & \text{for } \pm x<0\end{cases}, \tag{A4}$$

with $x_0=x_\pm$ for $\pm x_\pm>0$. For $\alpha'>0$, there is no (non-trivial) square-integrable solution to the homogeneous equation and hence a unique solution is obtained without the specification of any b.c.s. Focussing attention on the homogeneous problem, $(f\equiv 0)$, we note that for $\gamma>2|\alpha'|$ the solution is smooth; if $0<\gamma\le 2|\alpha'|$, u is continuous, whereas if $\alpha'<\gamma<0$ the solution is

singular at $x = 0$. For $\gamma = 0$, the solution could be continuous or discontinuous with a finite jump, depending upon the boundary conditions.

Friedrichs' (1958) classic, lengthy paper may be taken as evidence that the type of situation we are dealing with is not exceptional, not restricted to simple 1-d problems, and amenable to mathematical analysis. In describing the scope of his work in that paper, Friedrichs remarks: "The loss or gain of a boundary condition for the simple equation just considered [(A1)], which was read off from the explicit representation of the solution, can also be deduced from the general criteria to be formulated in this paper. From the same criteria, and in a closely analogous manner, we shall be able to derive a loss (or gain) of a boundary condition for the Tricomi equation and other partly elliptic, partly hyperbolic equations.

The elliptic or hyperbolic character of an equation is defined by algebraic conditions on its coefficients. The equations we shall study will be characterized by different algebraic conditions. We shall show that to each equation of this type a class of proper boundary conditions can be assigned. These conditions—and in particular the number of data involved in these conditions—depend only on the algebraic nature of the coefficients at the boundary."

In the context of the work presented in this paper, we note that the linearized equation (17) is a scalar first-order equation and hence trivially hyperbolic by any accepted definition of the term. With a dependence of hardening rate on $\nabla \boldsymbol{P}$ in the 3-d case, rate-dependent as well as rate-independent, the linearized evolution equations for $\boldsymbol{P}$ would seem to lack the symmetry required to be fitted into Friedrichs' framework of symmetric positive linear systems, but fall in the general category of linear first-order systems that have been studied in the mathematical literature. Furthermore, the equations of gradient plasticity are fundamentally nonlinear evolutionary problems. As such, they appear to provide a rich source of challenges to the interested mathematical analyst.

Figure Captions

Figure 1. Sketch of plastic strain gradient and strain for a) $-S_- = S_+ = S > 0$, b) $S_- = -S_+ = S > 0$, $|B/A|L < 2/S$.

Figure 2. An infinite layer of material bonded to two rigid platens under simple shear deformation. The bottom suface of the layer is held fixed and a shear traction is applied to the top surface.

Figure 3. Plastic strain profiles for initially upward parabolic distribution: (a) $k_0 b/H = 2\times10^{-3}$, and (b) $k_0 b/H = 2\times10^{-4}$. In the calculations, boundary condition 2 (see step 7 b in the numerical algorithm of Sec. 4) is used where gradient effects are ignored on the boundaries and $\Delta g = 5\times10^{-8} g_0$.

Figure 4. Plastic strain for initially upward parabolic distribution with no boundary condition imposed. $k_0 b/H = 2\times10^{-3}$ and $\Delta g = 5\times10^{-8} g_0$.

Figure 5. Convergence of plastic strain profiles with respect to spatial discretization for initially upward parabolic distribution and without boundary conditions; $k_0 b/H = 2\times10^{-3}$, EL stands for the number of elements used.

Figure 6. Plastic strain profiles for initially downward parabolic distribution: (a) $k_0 b/H = 2\times10^{-3}$, and (b) $k_0 b/H = 2\times10^{-5}$. No boundary conditions are necessary and $\Delta g = 5\times10^{-8} g_0$.

Figure 7. Plastic strain profiles for initially exponential distribution: (a) $k_0 b/H = 2\times10^{-3}$, and (b) $k_0 b/H = 2\times10^{-5}$. No plastic strain boundary conditions are employed and $\Delta g = 5\times10^{-8} g_0$.

Figure 8. Convergence of plastic strain profiles with respect to spatial and temporal discretization at $g/g_0 = 1.0025$ for $k_0 b/H = 2\times10^{-3}$. (a) initially downward parabolic distribution, and (b) initially upward parabolic distribution. EL stands for number of elements used.

Figure 9. Comparison of solutions on half and full-domain for initially upward parabolic distribution of plastic strain with $k_0 b/H = 2\times10^{-3}$.

Figure 10. Plastic strain profiles with constrained boundary conditions (zero plastic strain) and with zero initial plastic strain. (a) $k_0 b/H = 2\times10^{-3}$, (b) $k_0 b/H = 2\times10^{-5}$. Variation of boundary layer thickness with respect to k_0 at (c) fixed applied displacement of $u_2/H = 0.008$ and (d) fixed applied load of $g/g_0 = 1.1$. Figure (e) displays stress-strain curves for various values of $k_0 b/H$.

Figure 11. Displacement profiles corresponding to Fig. 10(a).

Figure 12. Plastic strain profiles for initially symmetric, piece-wise linear distribution. Plastic strains at the boundaries are constrained.

Figure 13. Plastic strain profiles for initially linear distribution. Plastic strains at the boundaries are constrained.

Figure 14. Plastic strain profiles for initially upward parabolic distribution and hardening according to Eqn. (28), with no boundary condition imposed.

Figure 15. Plastic strain profile for initially upward parabolic distribution with hardening according to Eqn. (29), with no boundary condition imposed.

Figure 16. a) Result corresponding to Figure 4 with hardening according to Eqn. (30); b) Result corresponding to Figure 10(b) with hardening according to Eqn. (30); c) Plastic strain profiles for initially upward parabolic distribution with hardening according to Eqn. (31) and no b.c.s applied.

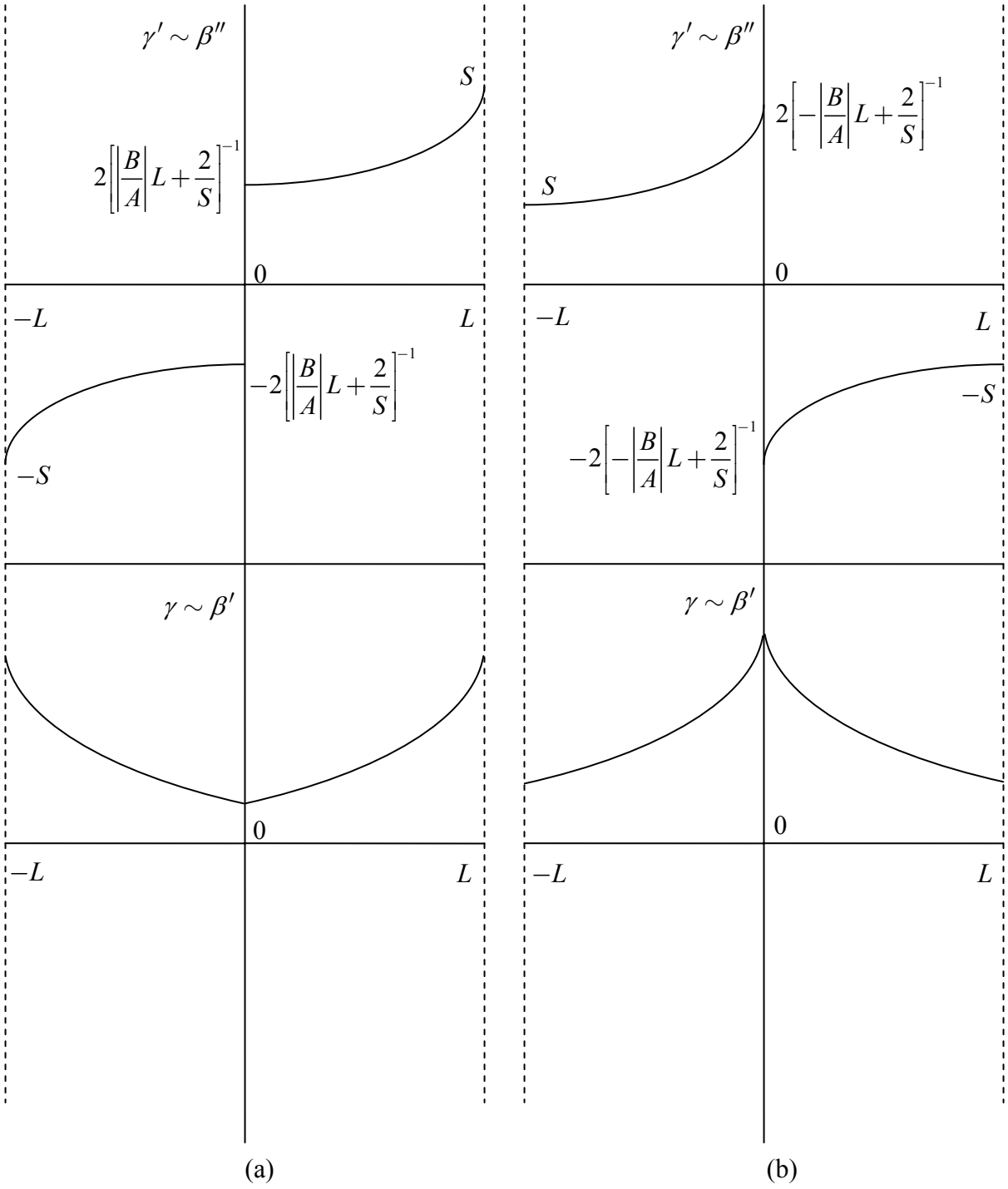

Figure 1. Sketch of plastic strain gradient and strain for a) $-S_{-}=S_{+}=S>0$, b) $S_{-}=-S_{+}=S>0$, $\left|B/A\right|L<2/S$.

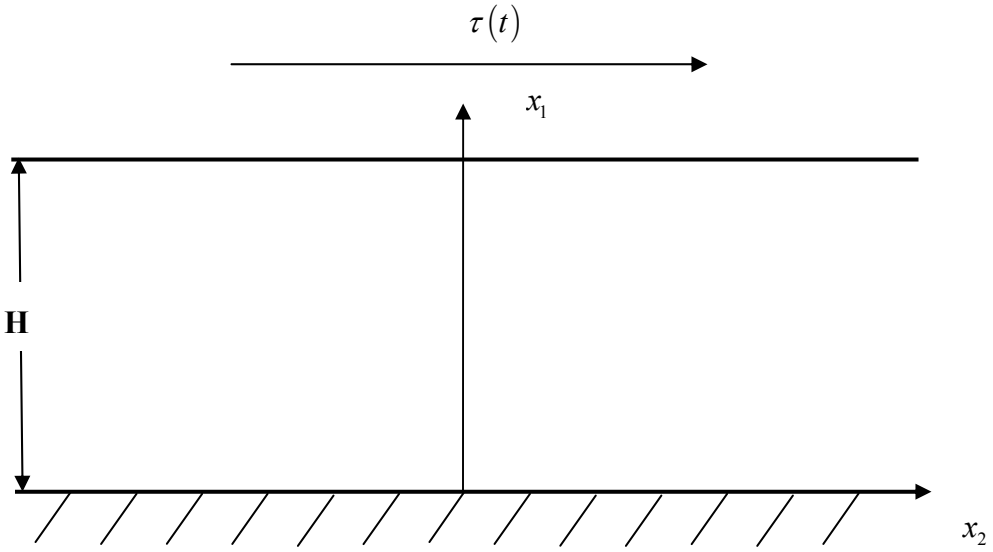

Figure 2. An infinite layer of material bonded to two rigid platens under simple shear deformation. The bottom suface of the layer is held fixed and a shear traction is applied to the top surface.

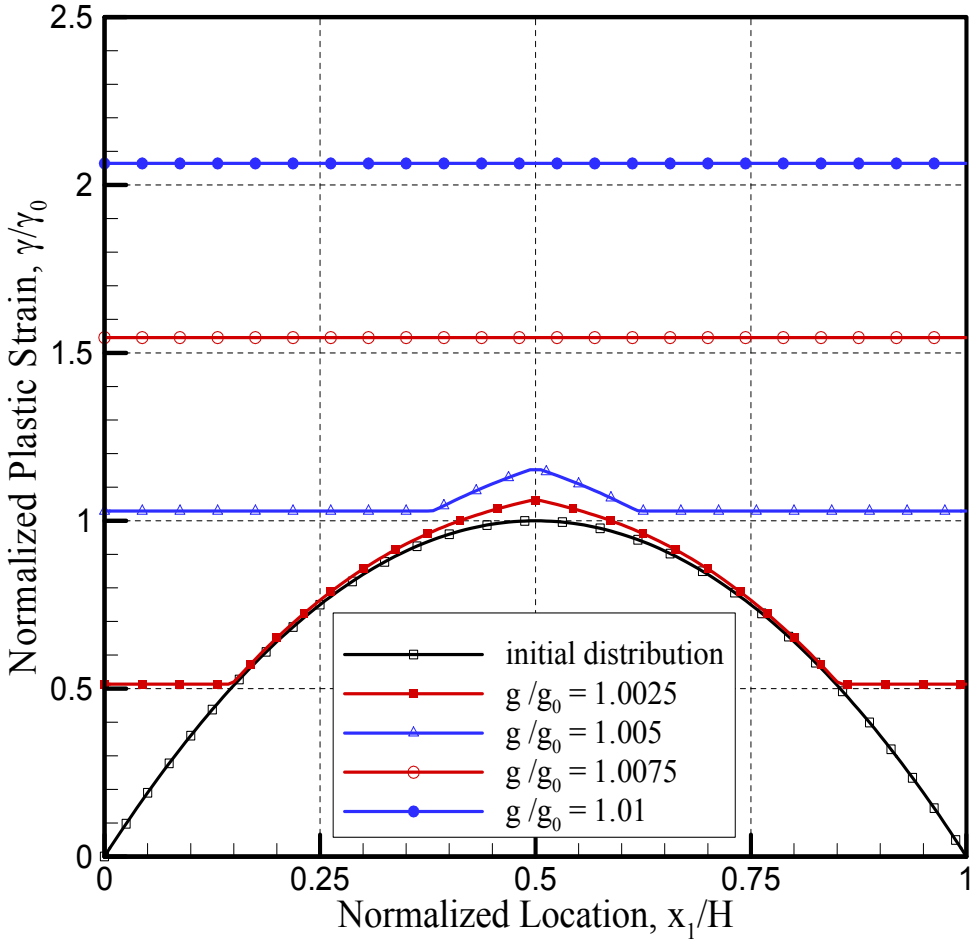
2.5
2
1.5
1
0.5
0
0
0.25
0.5
0.75
1
Normalized Plastic Strain, γ/γ0
Normalized Location, x1/H
initial distribution
g /g0 = 1.0025
g /g0 = 1.005
g /g0 = 1.0075
g /g0 = 1.01

3 (a)

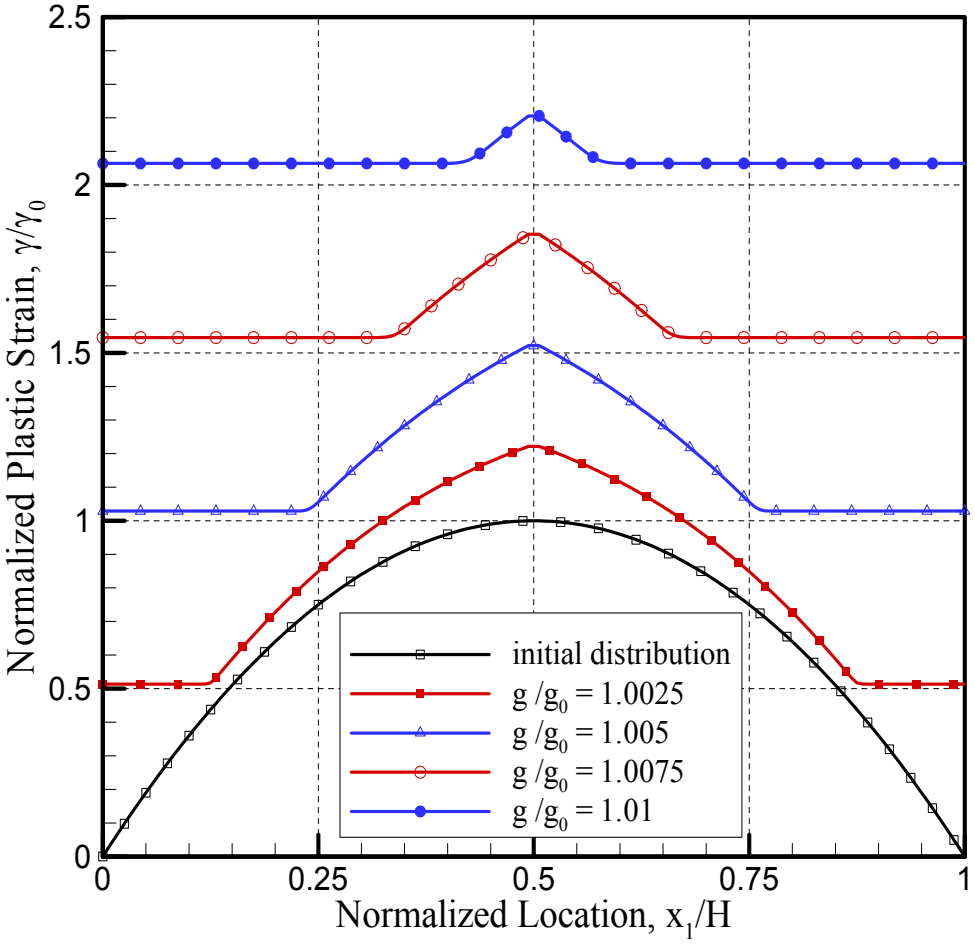

3 (b)

Figure 3. Plastic strain profiles for initially upward parabolic distribution: (a) $k_0 b/H = 2\times10^{-3}$, and (b) $k_0 b/H = 2\times10^{-4}$. In the calculations, boundary condition 2 (see step 7b in the numerical algorithm of Section 4) is employed and $\Delta g = 5\times10^{-8} g_0$.

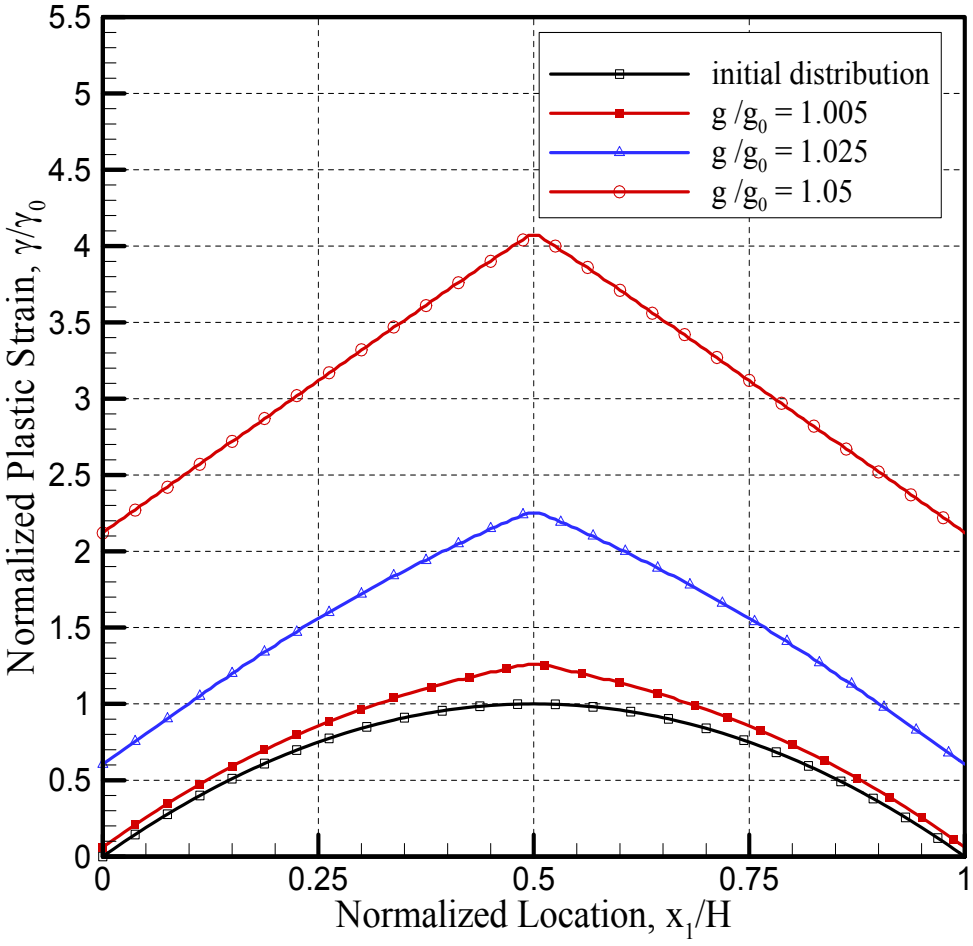

Figure 4. Plastic strain for initially upward parabolic distribution with no boundary condition imposed. $k_0 b/H = 2\times10^{-3}$ and $\Delta g = 5\times10^{-8} g_0$.

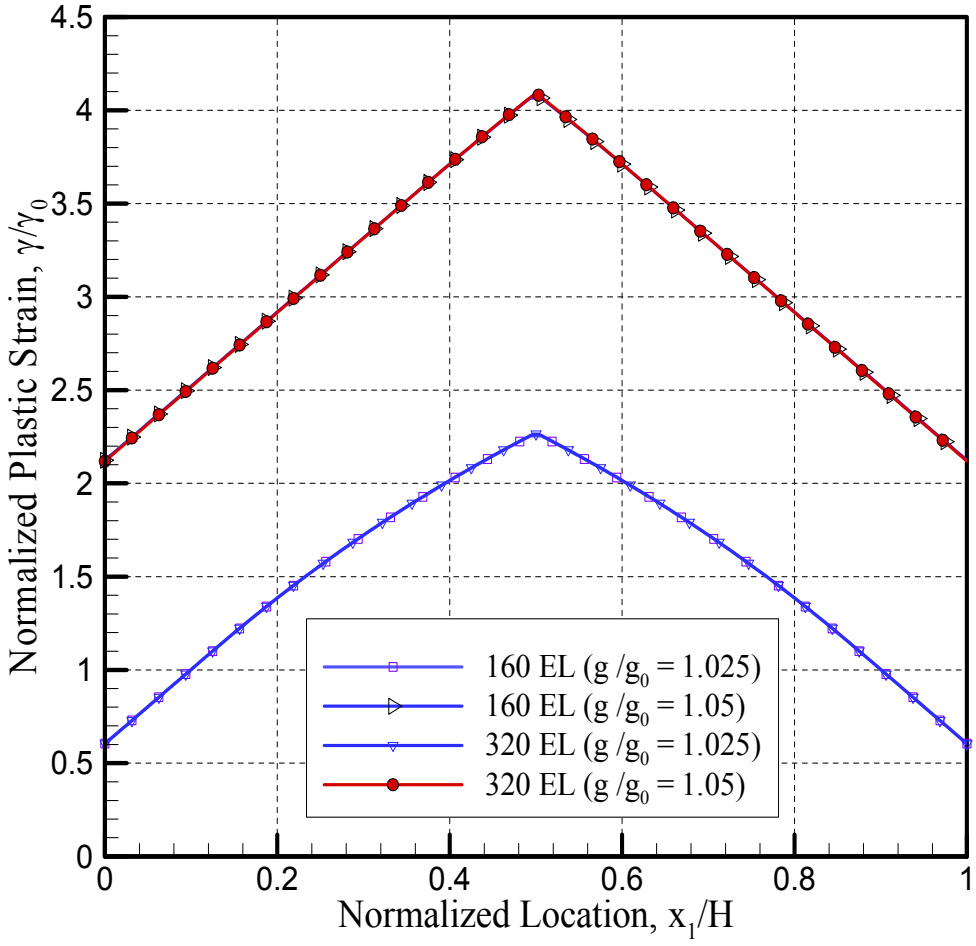

Figure 5. Convergence of plastic strain profiles with respect to spatial discretization for initially upward parabolic distribution and without boundary conditions; $k_0 b/H = 2\times10^{-3}$, EL stands for the number of elements used.

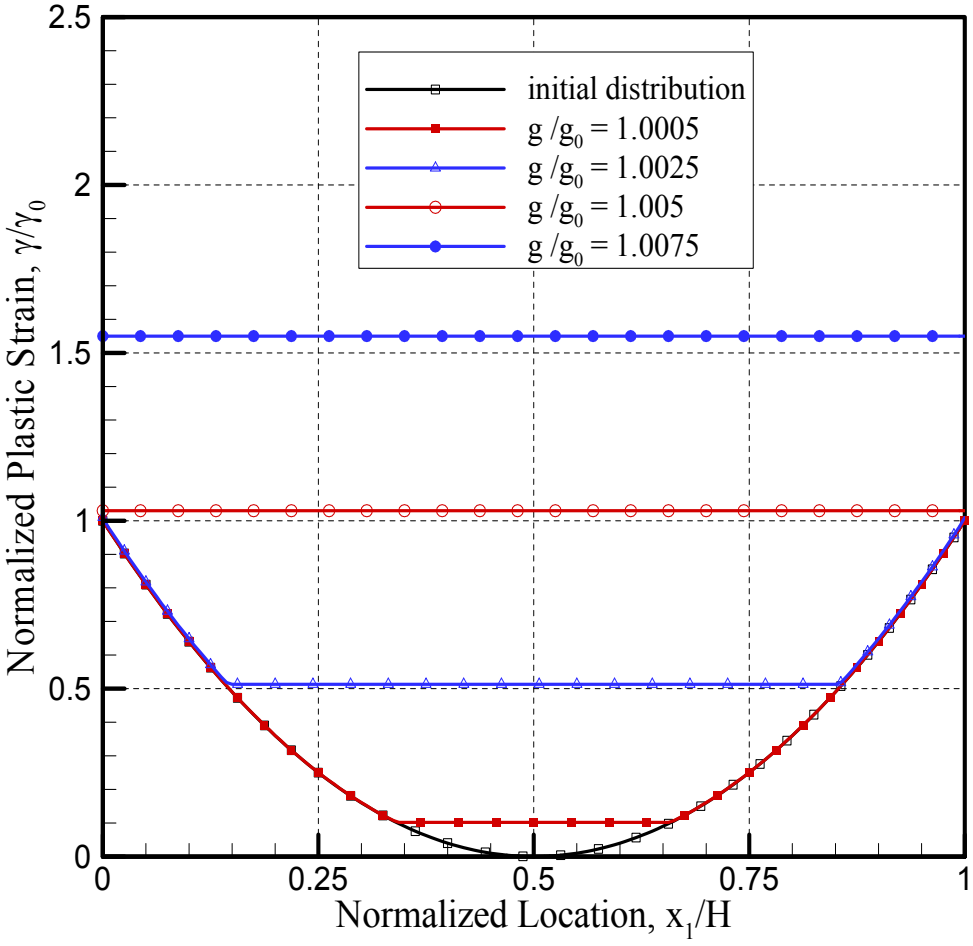
initial distribution
g /g0 = 1.0005
g /g0 = 1.0025
g /g0 = 1.005
g /g0 = 1.0075
Normalized Plastic Strain, γ/γ0
Normalized Location, x1/H
0
0.25
0.5
0.75
1
0
0.5
1
1.5
2
2.5

6 (a)

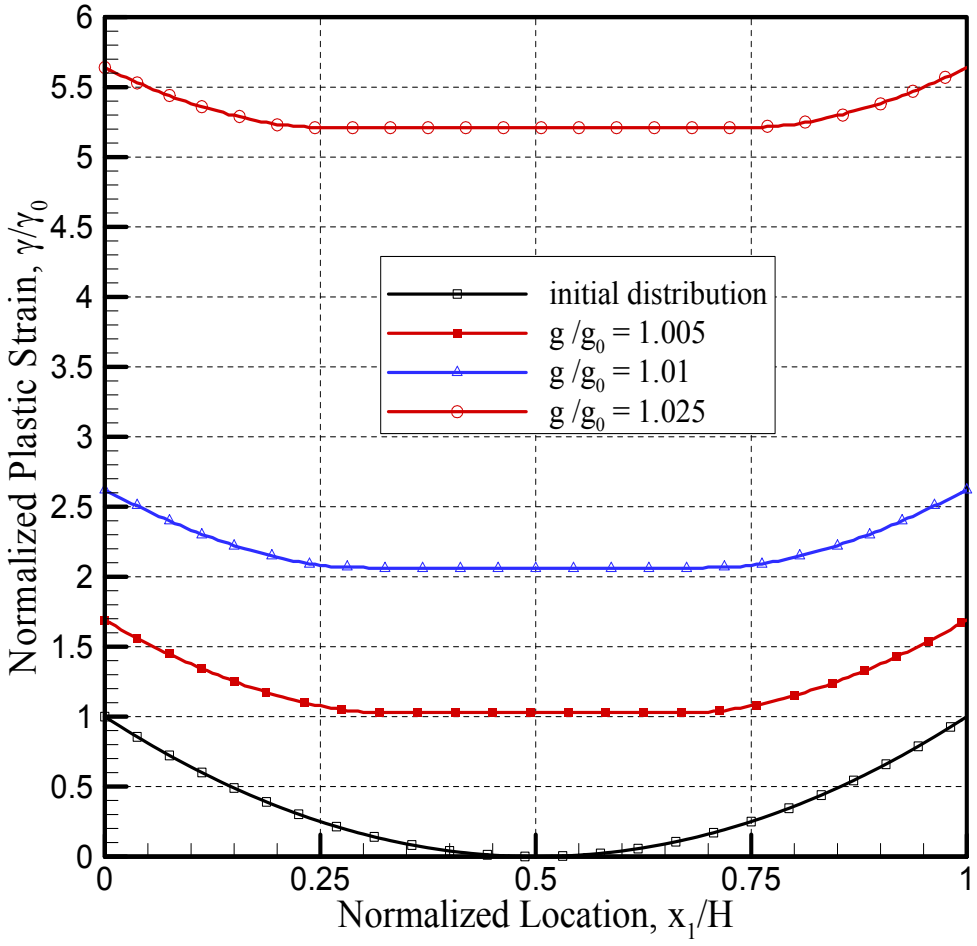

6 (b)

Figure 6. Plastic strain profiles for initially downward parabolic distribution: (a) $k_0 b/H = 2\times10^{-3}$, and (b) $k_0 b/H = 2\times10^{-5}$. No boundary conditions are necessary and $\Delta g = 5\times10^{-8} g_0$.

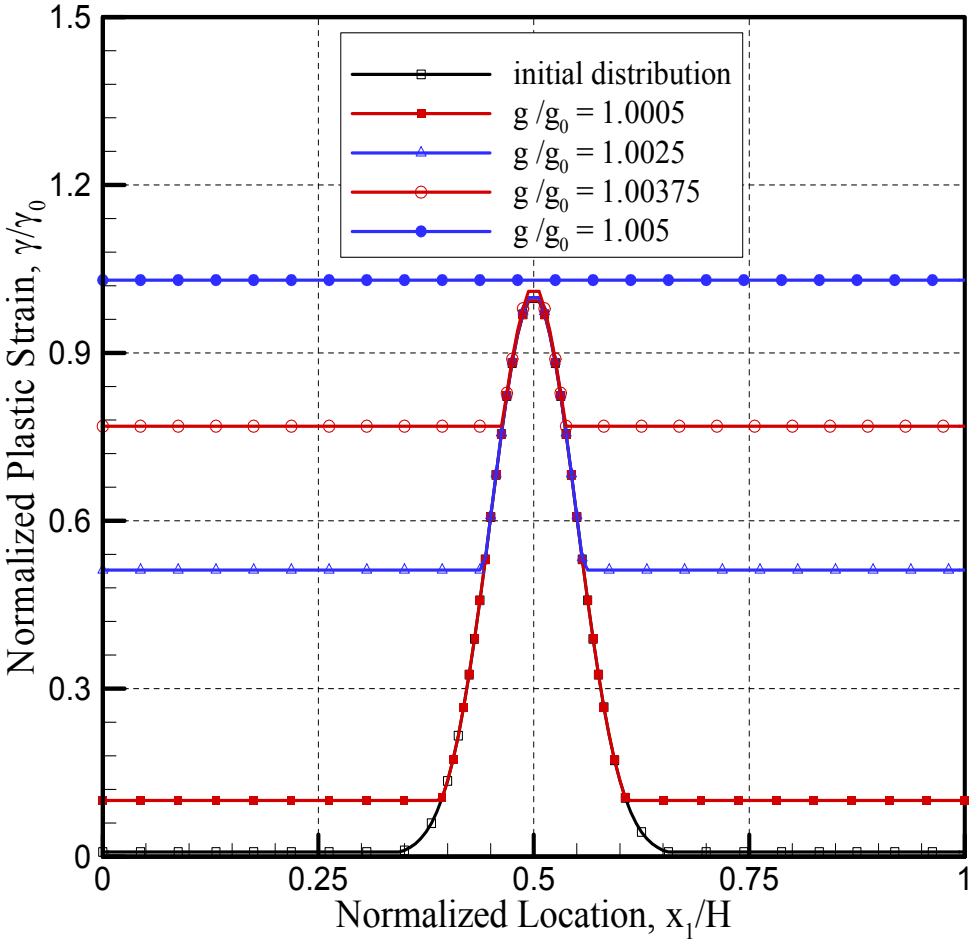
initial distribution
g /g0 = 1.0005
g /g0 = 1.0025
g /g0 = 1.00375
g /g0 = 1.005
Normalized Plastic Strain, γ/γ0
Normalized Location, x1/H
0
0.3
0.6
0.9
1.2
1.5
0.25
0.5
0.75
1

7 (a)

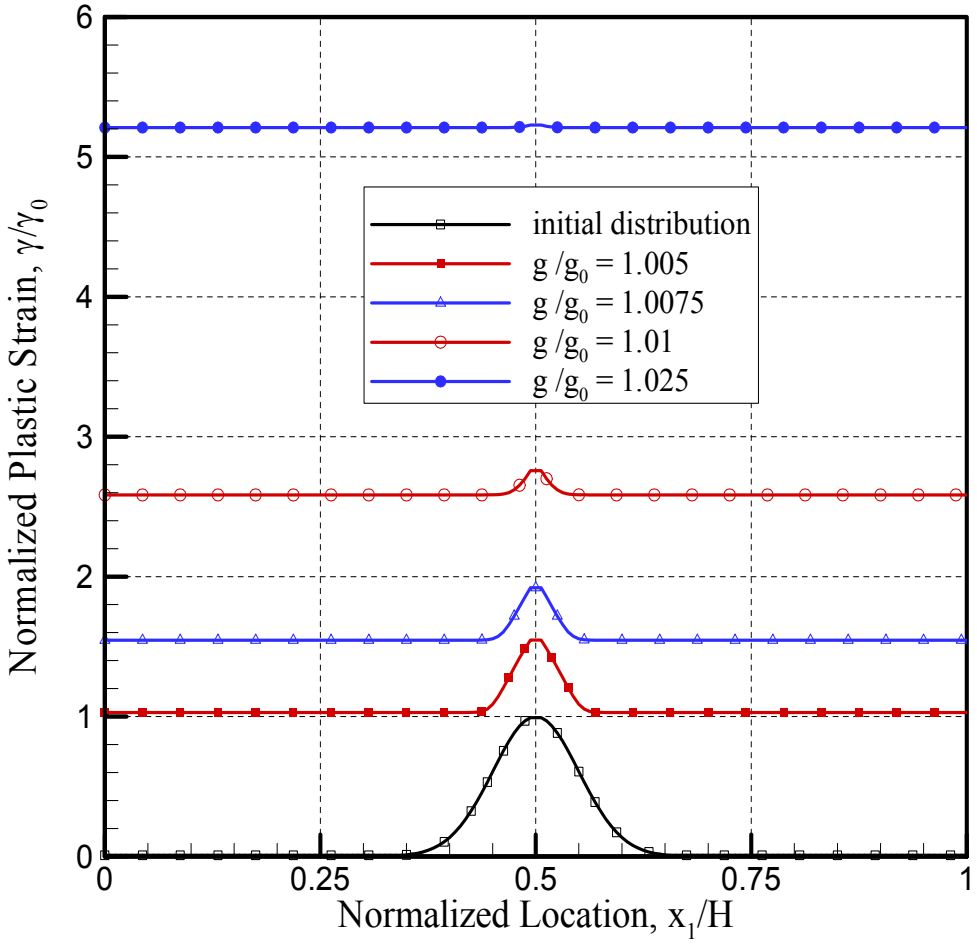

7 (b)

Figure 7. Plastic strain profiles for initially exponential distribution: (a) $k_0 b/H = 2\times10^{-3}$, and (b) $k_0 b/H = 2\times10^{-5}$. No plastic strain boundary conditions are employed and $\Delta g = 5\times10^{-8} g_0$.

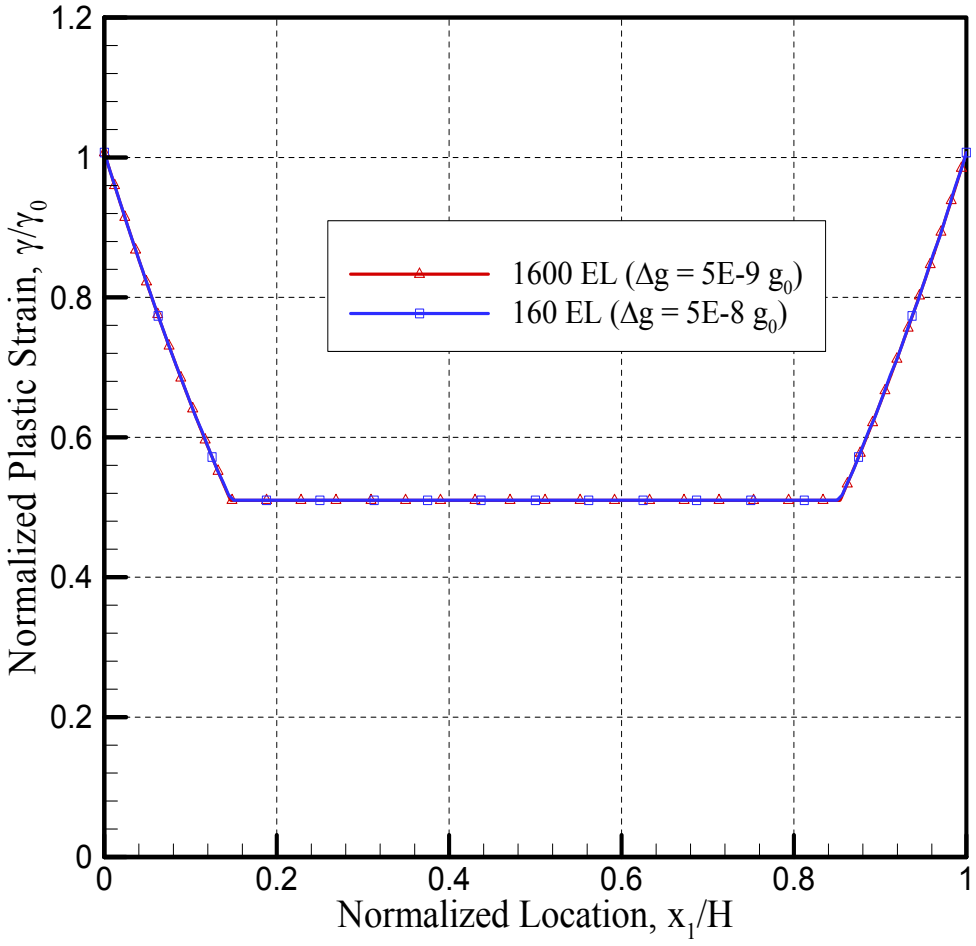
1.2
1
0.8
0.6
0.4
0.2
0
0
0.2
0.4
0.6
0.8
1
Normalized Plastic Strain, γ/γ0
Normalized Location, x1/H
1600 EL (Δg = 5E-9 g0)
160 EL (Δg = 5E-8 g0)

8 (a)

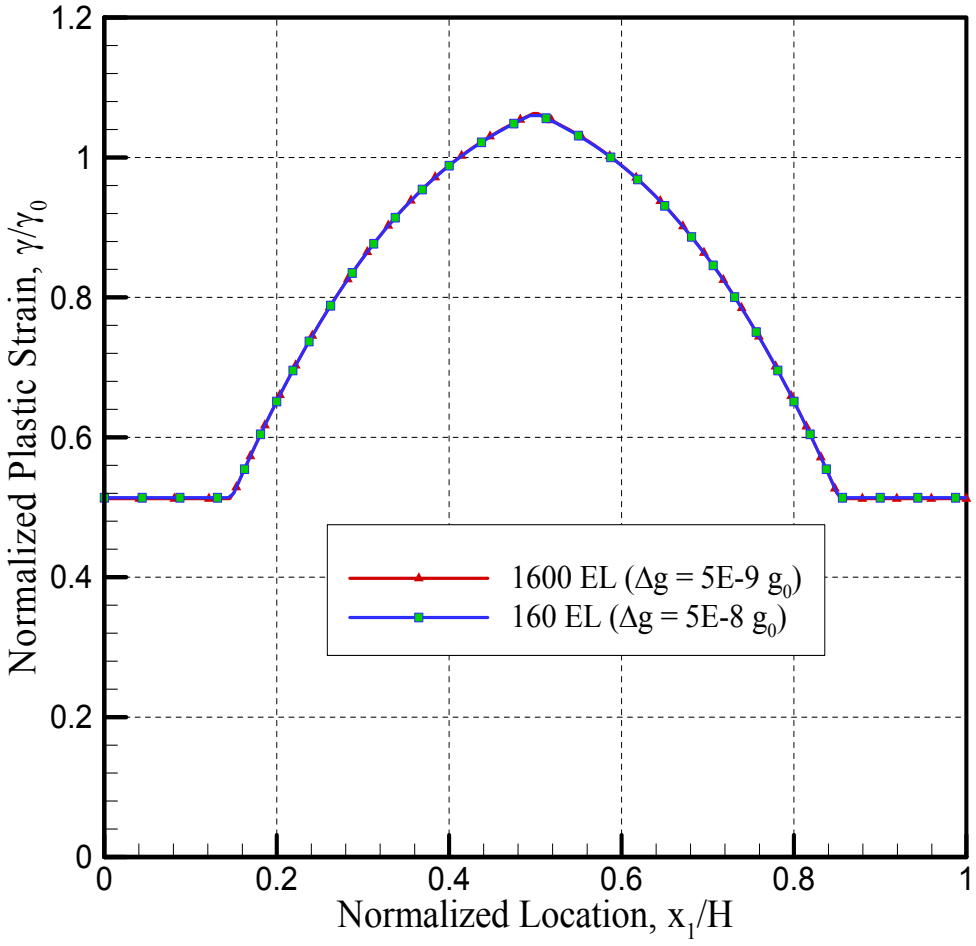

8 (b)

Figure 8. Convergence of plastic strain profiles with respect to spatial and temporal discretization at $g/g_0 = 1.0025$ for $k_0 b/H = 2\times10^{-3}$. (a) initially downward parabolic distribution, and (b) initially upward parabolic distribution. EL stands for number of elements used.

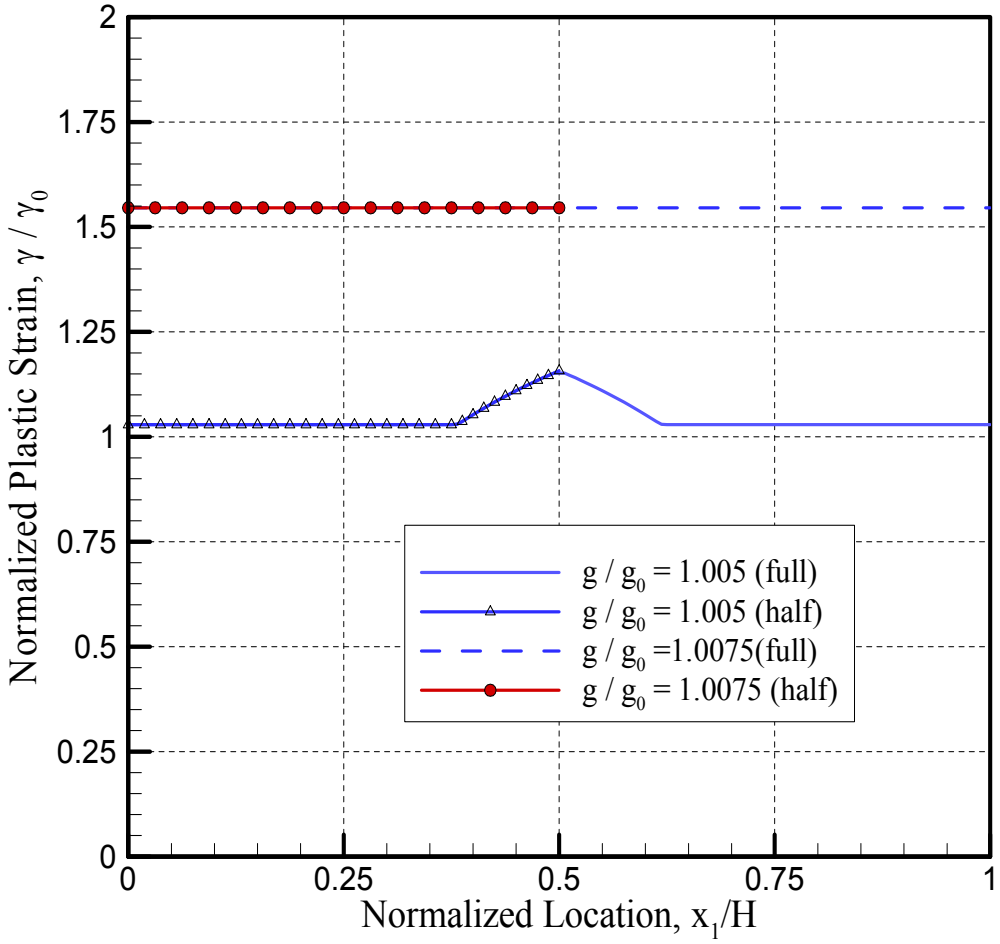

Figure 9. Comparison of solutions on half and full-domain for initially upward parabolic distribution of plastic strain with $k_0 b/H = 2\times10^{-3}$.

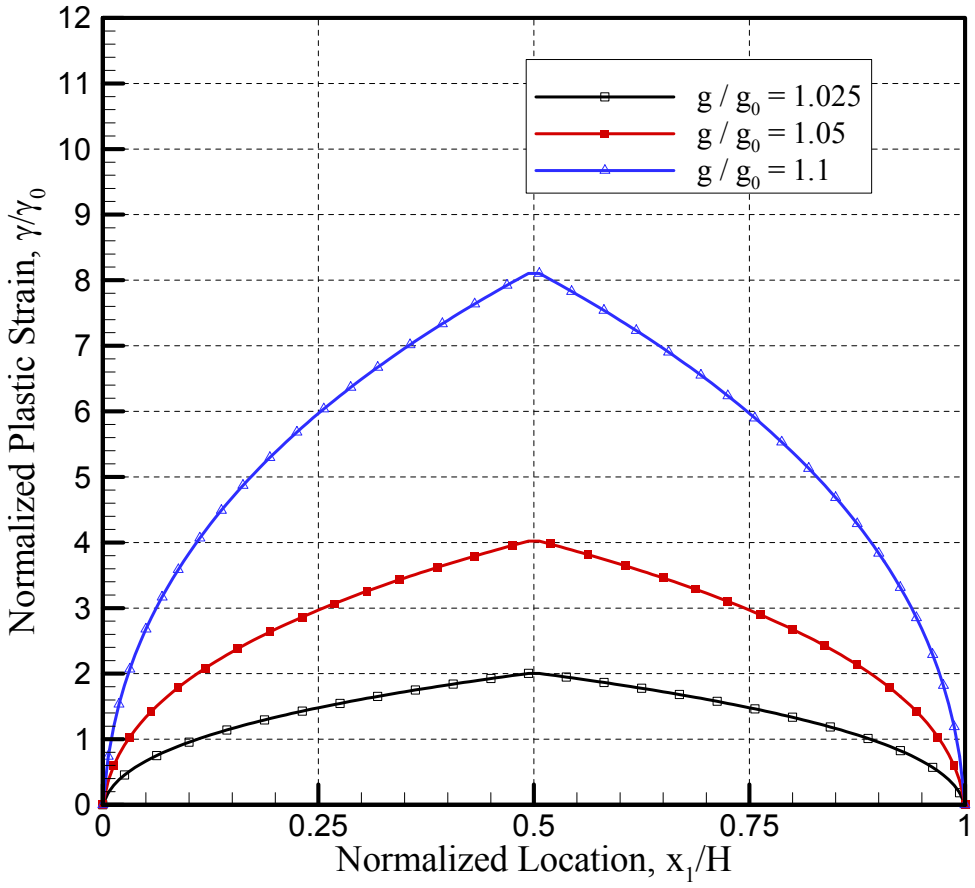
g / g0 = 1.025
g / g0 = 1.05
g / g0 = 1.1
Normalized Plastic Strain, γ/γ0
Normalized Location, x1/H
0
1
2
3
4
5
6
7
8
9
10
11
12
0
0.25
0.5
0.75
1

10 (a)

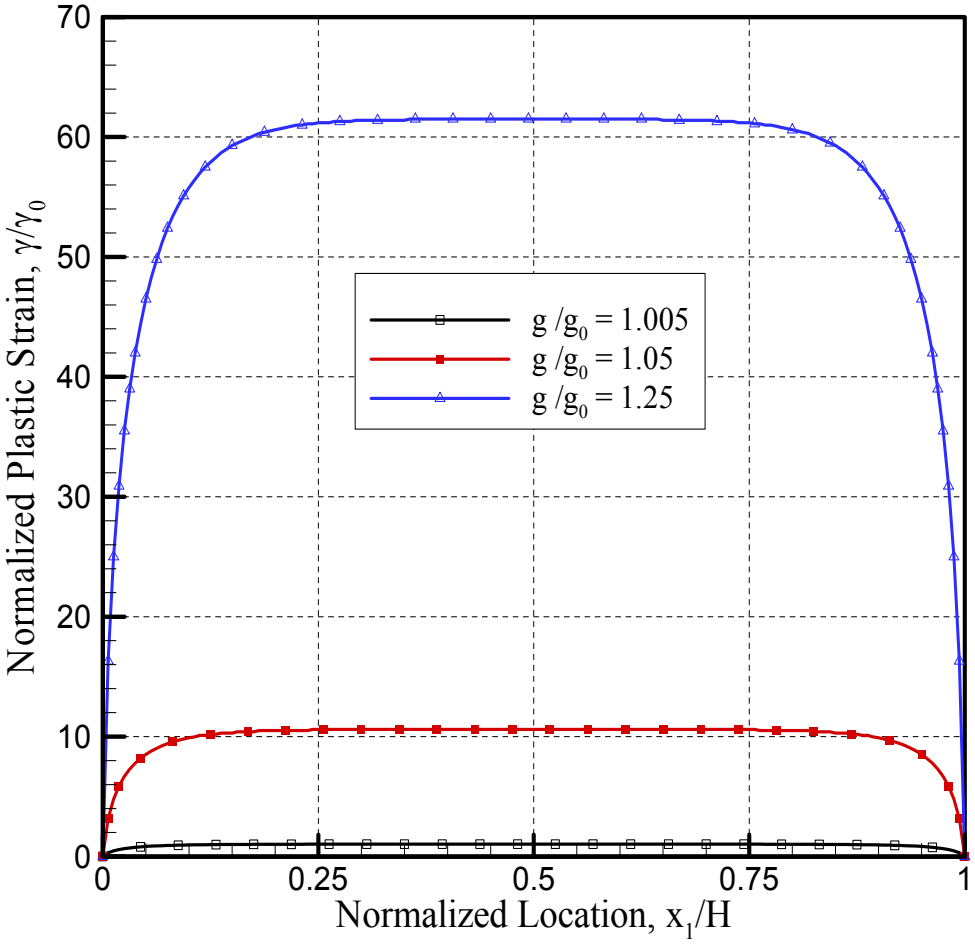
70
60
50
40
30
20
10
0
0
0.25
0.5
0.75
1
Normalized Plastic Strain, γ/γ0
Normalized Location, x1/H
g /g0 = 1.005
g /g0 = 1.05
g /g0 = 1.25

10 (b)

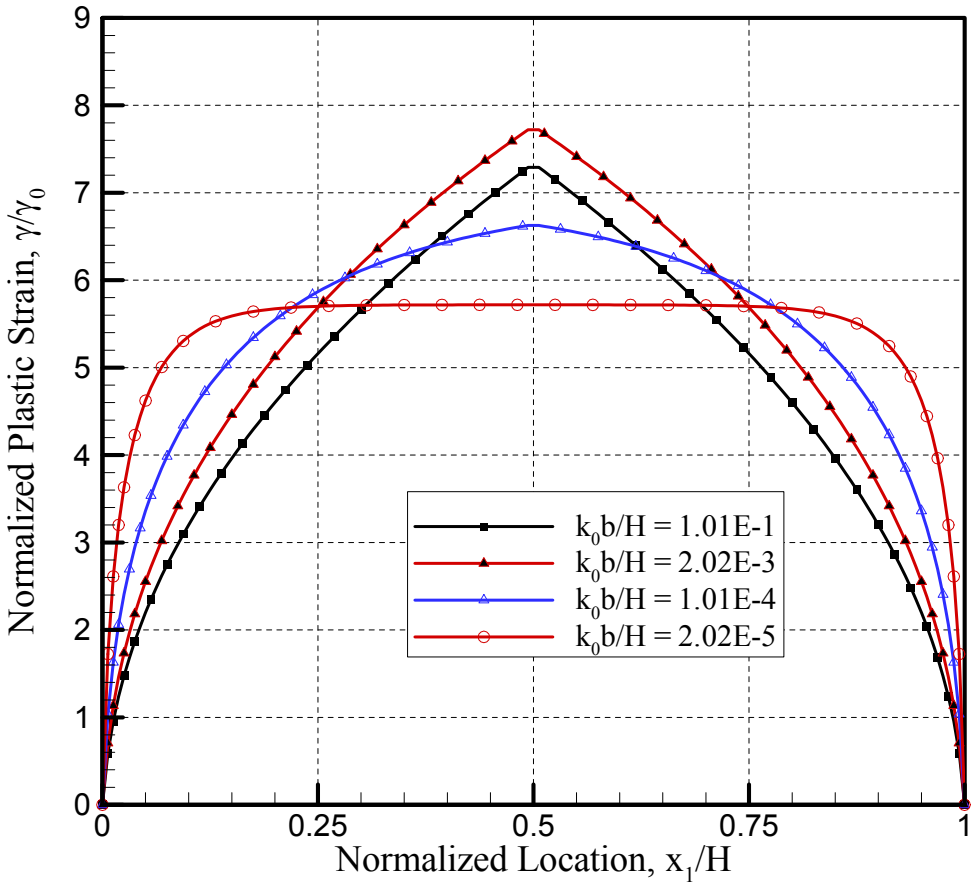
Normalized Plastic Strain, γ/γ_0
Normalized Location, x_1/H
k_0b/H = 1.01E-1
k_0b/H = 2.02E-3
k_0b/H = 1.01E-4
k_0b/H = 2.02E-5
0
1
2
3
4
5
6
7
8
9
0
0.25
0.5
0.75
1

10 (c)

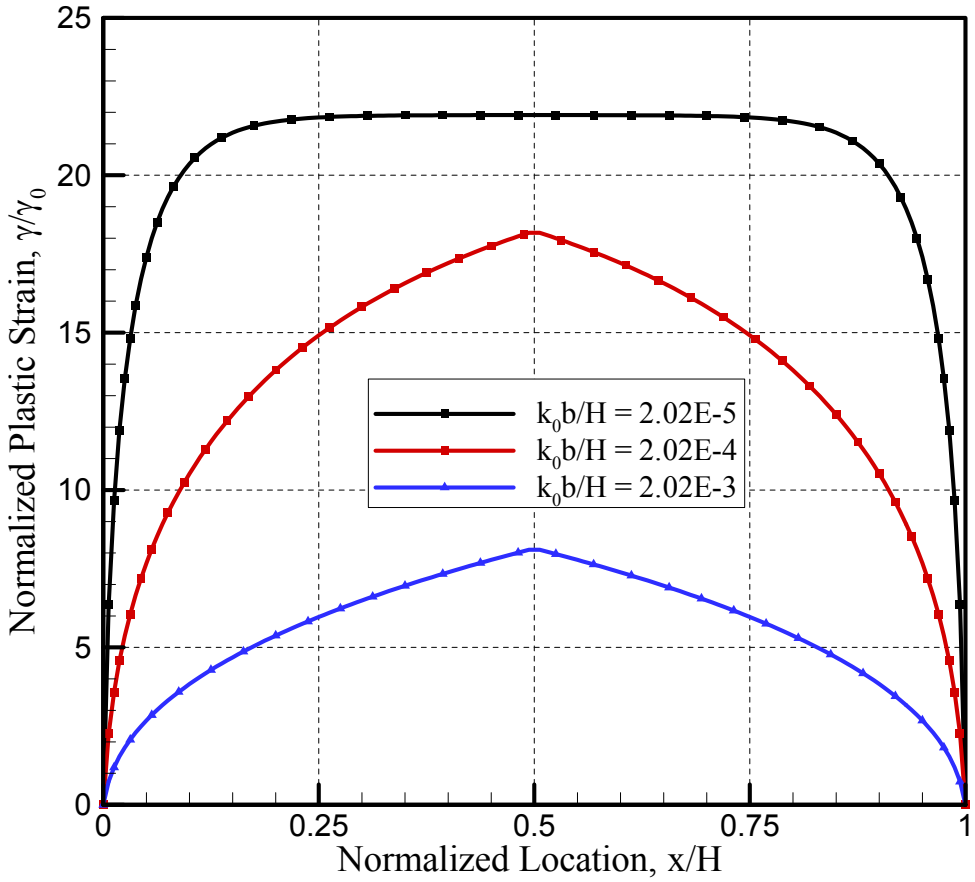
25
20
15
10
5
0
0
0.25
0.5
0.75
1
Normalized Plastic Strain, γ/γ0
Normalized Location, x/H
k0b/H = 2.02E-5
k0b/H = 2.02E-4
k0b/H = 2.02E-3

10(d)

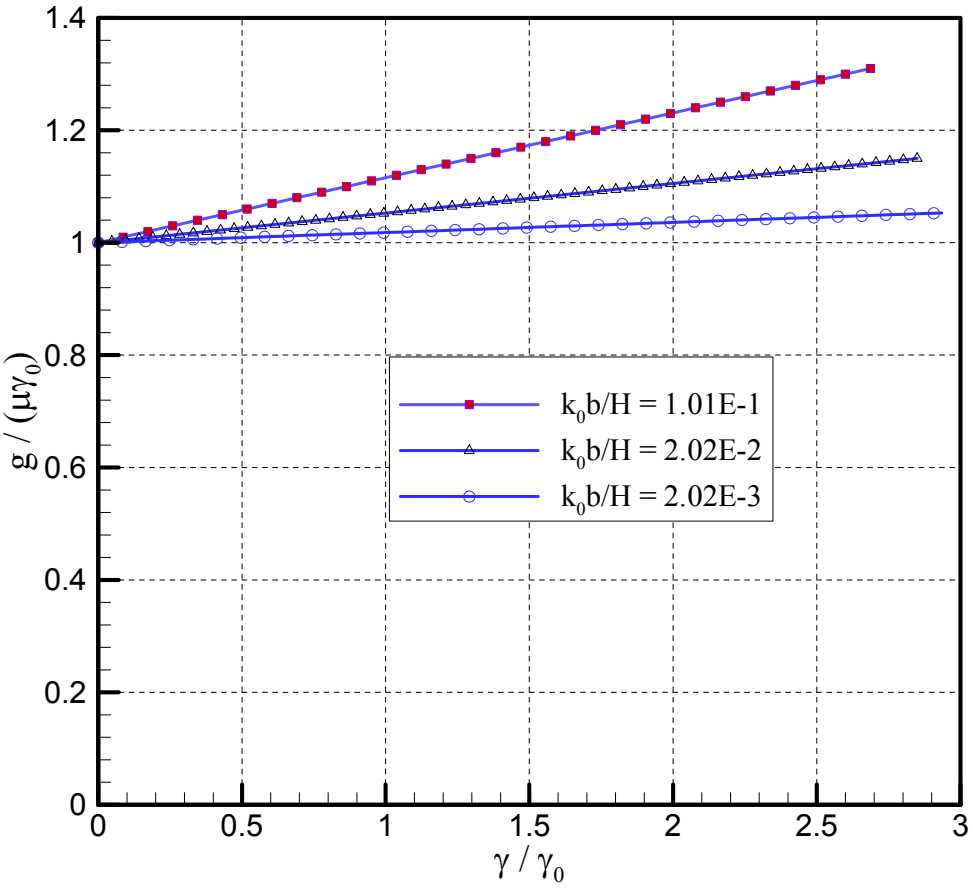

10(e)

Figure 10. Plastic strain profiles with constrained boundary conditions and without initial plastic strain. (a) $k_0 b/H = 2\times10^{-3}$, (b) $k_0 b/H = 2\times10^{-5}$. Variation of boundary layer thickness with respect to k_0 at (c) fixed applied displacement of $u_2/H = 0.008$ and (d) fixed applied load of $g/g_0 = 1.1$. Figure (e) displays stress-strain curves for various values of $k_0 b/H$.

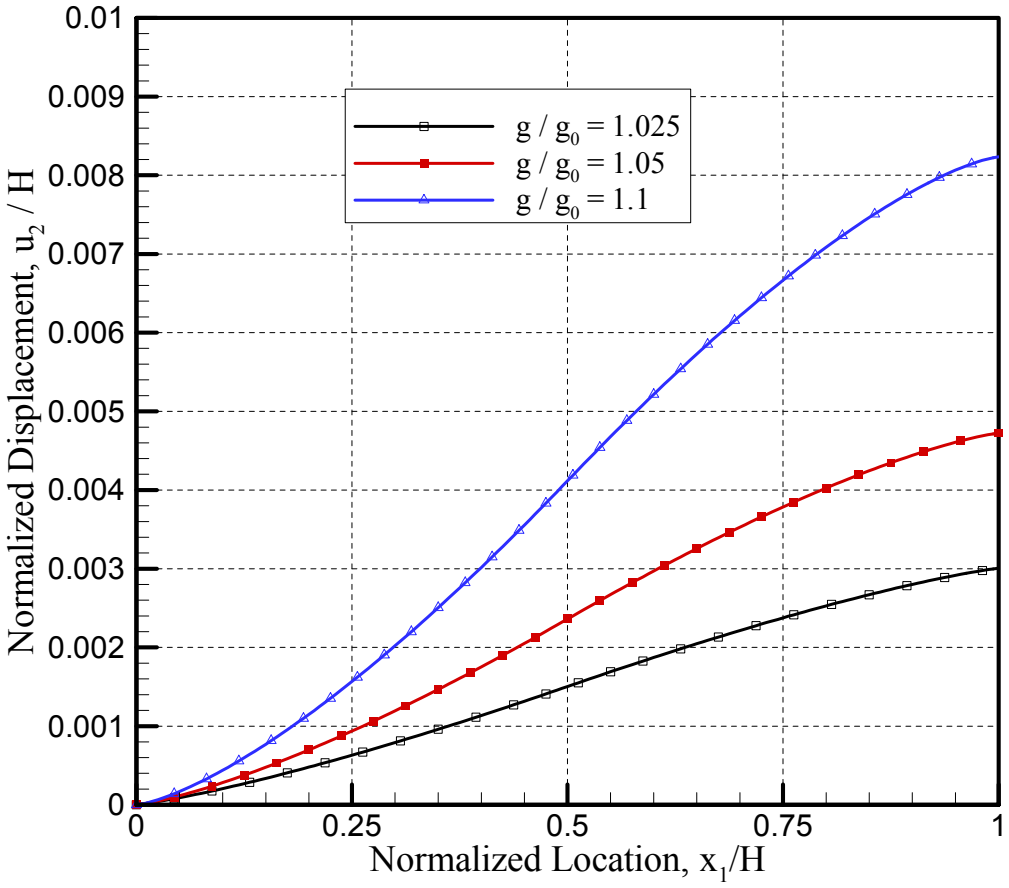

Figure 11. Displacement profiles corresponding to Fig. 10(a).

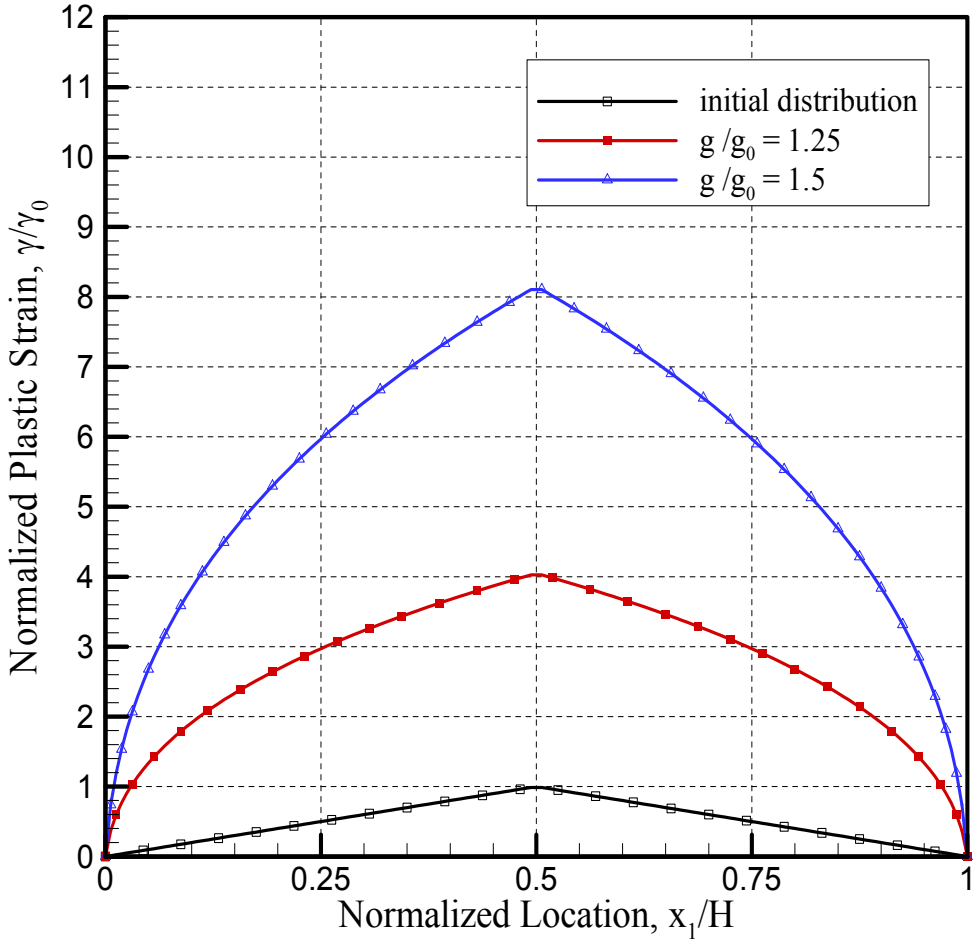

Figure 12. Plastic strain profiles for initially symmetric, piece-wise linear distribution. Plastic strains at the boundaries are constrained.

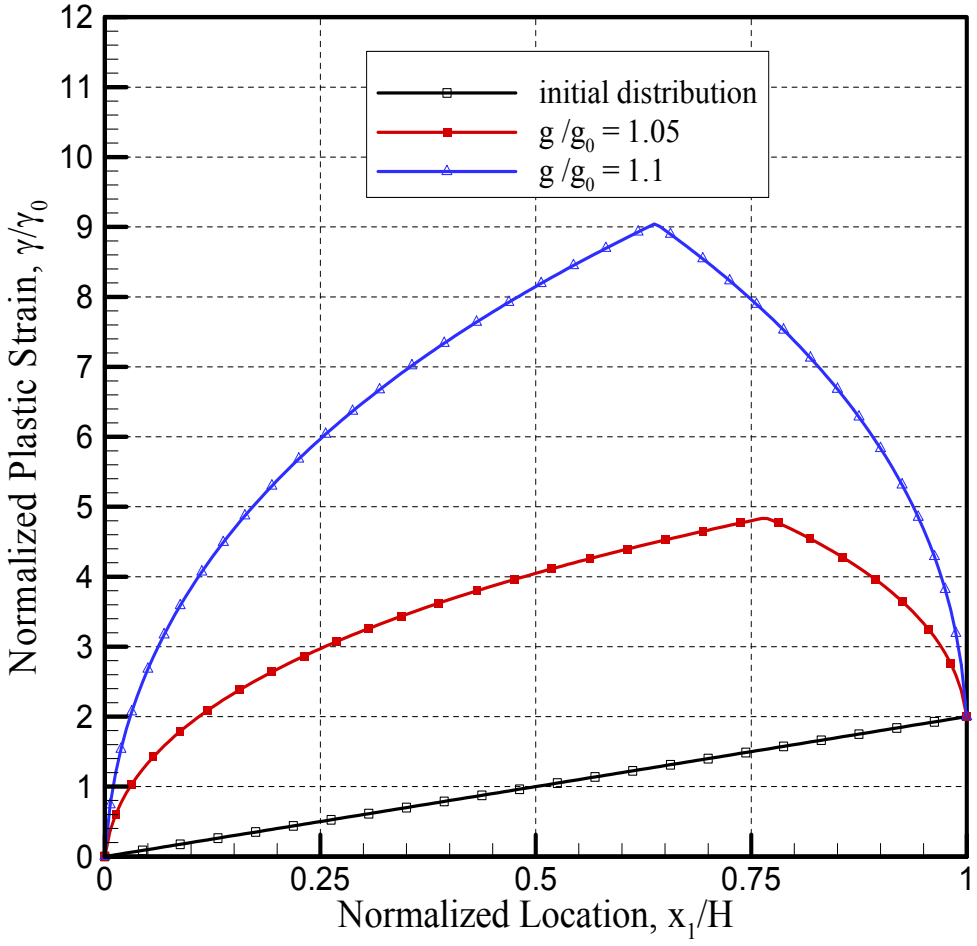

Figure 13. Plastic strain profiles for initially linear distribution. Plastic strains at the boundaries are constrained.

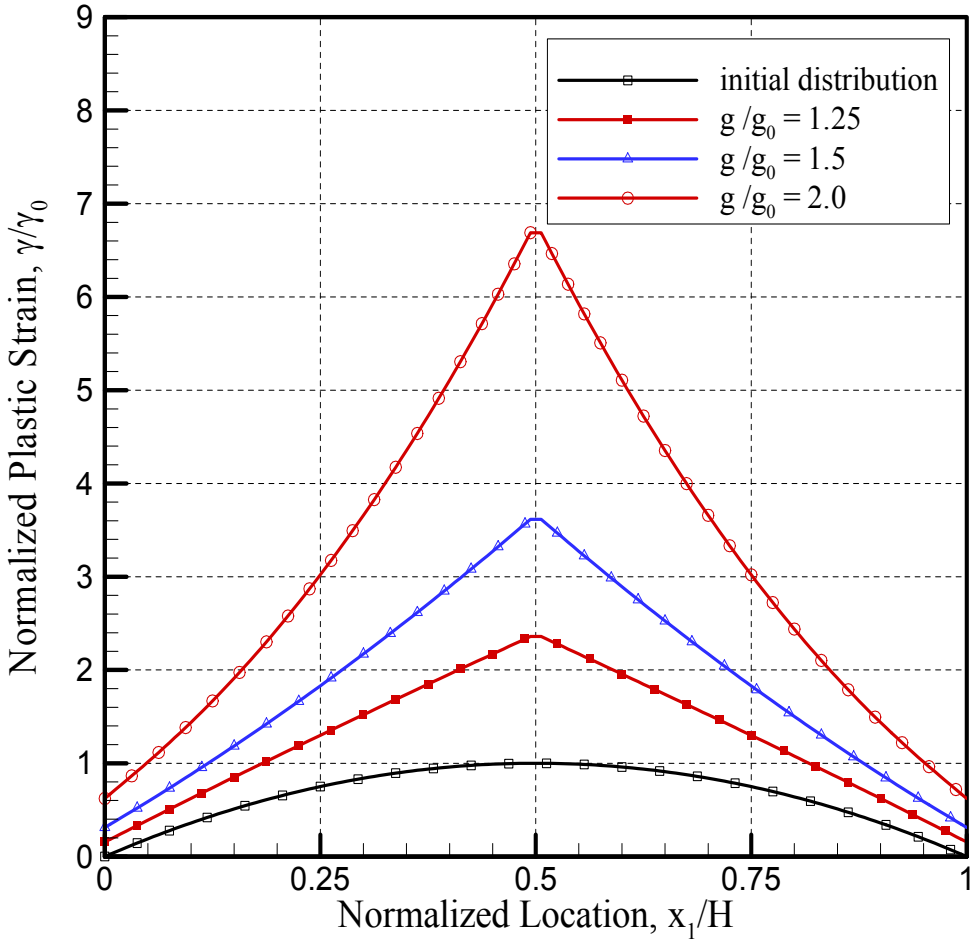

Figure 14. Plastic strain profiles for initially upward parabolic distribution and hardening according to Eqn. (28), with no b.c.s imposed.

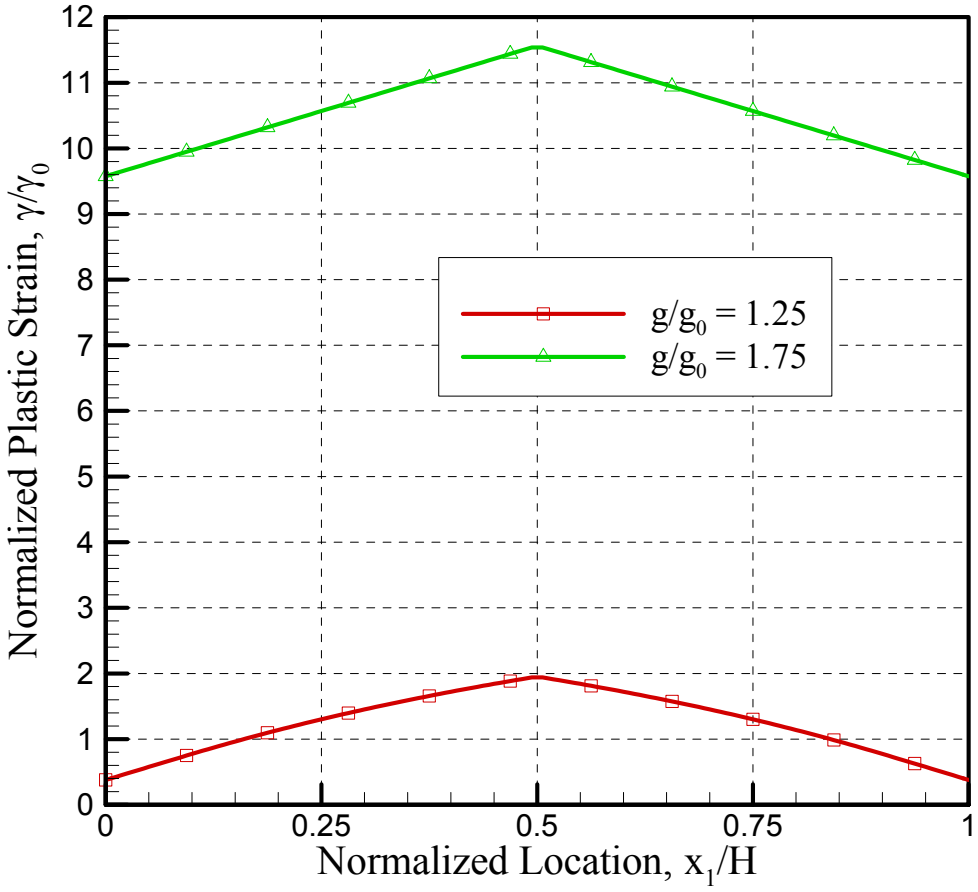

Figure 15. Plastic strain profile for initially upward parabolic distribution and hardening according to Eqn. (29), with no b.c.s imposed.

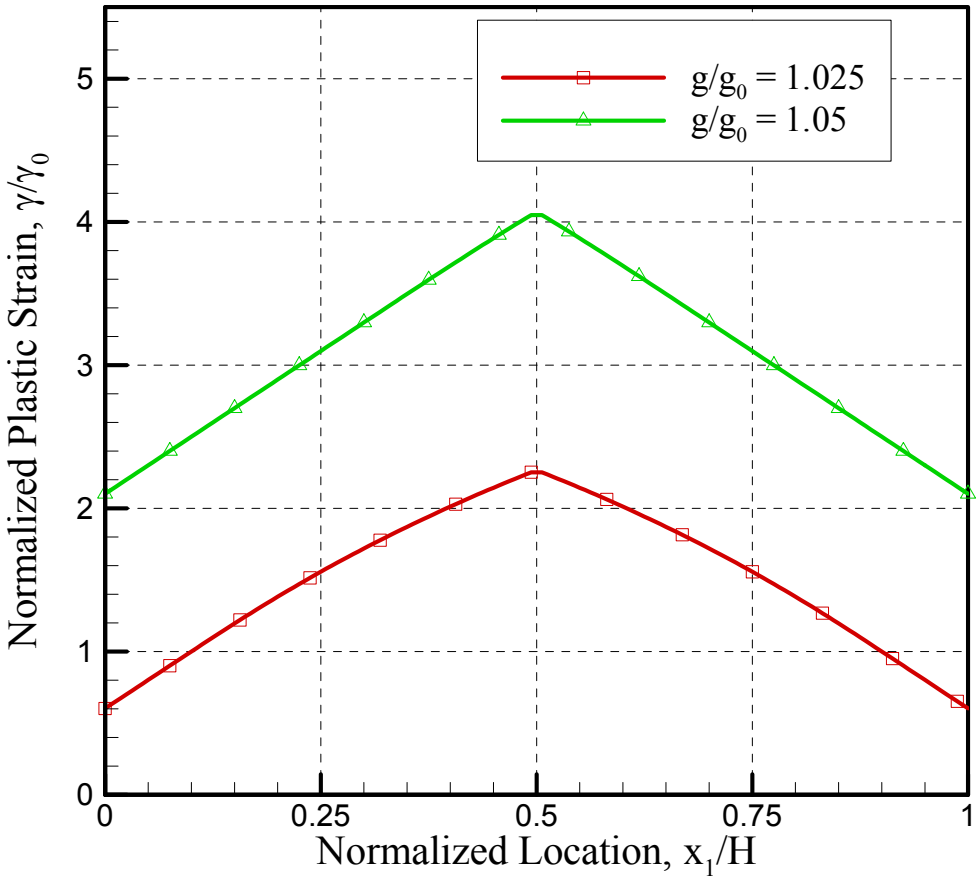
g/g0 = 1.025
g/g0 = 1.05
Normalized Plastic Strain, γ/γ0
Normalized Location, x1/H
0
1
2
3
4
5
0
0.25
0.5
0.75
1

16 (a)

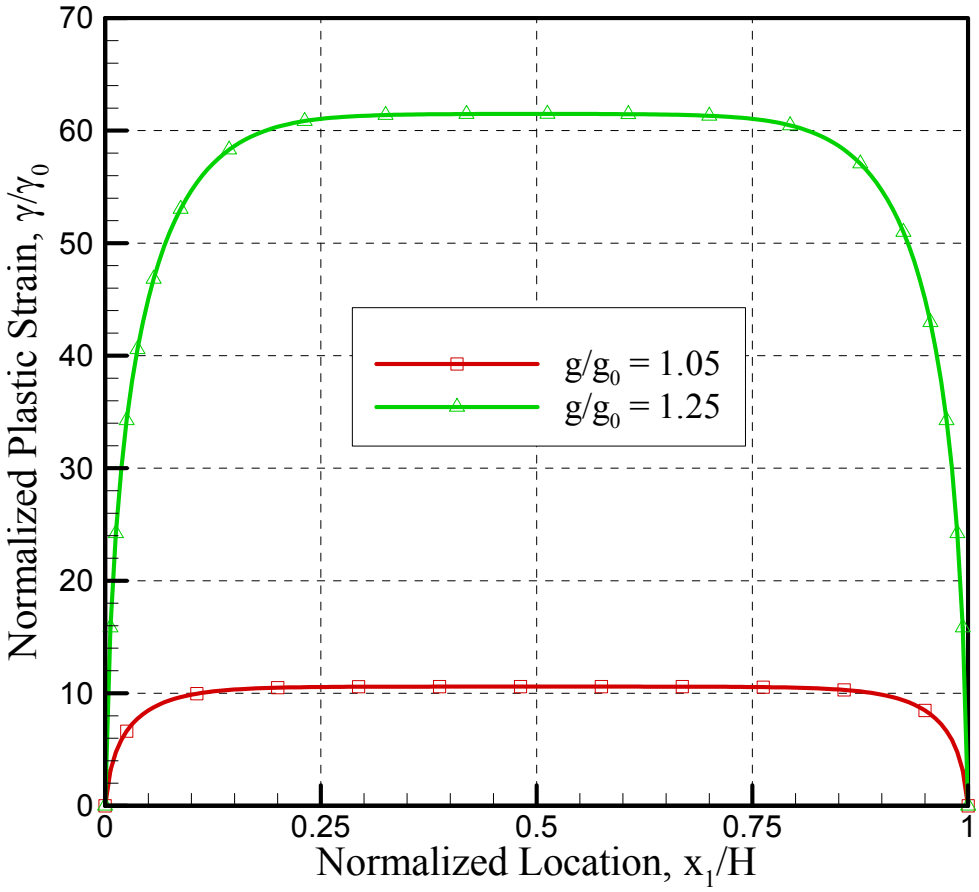
Normalized Plastic Strain, γ/γ_0
Normalized Location, x_1/H
$g/g_0 = 1.05$
$g/g_0 = 1.25$
0
10
20
30
40
50
60
70
0
0.25
0.5
0.75
1

16 (b)

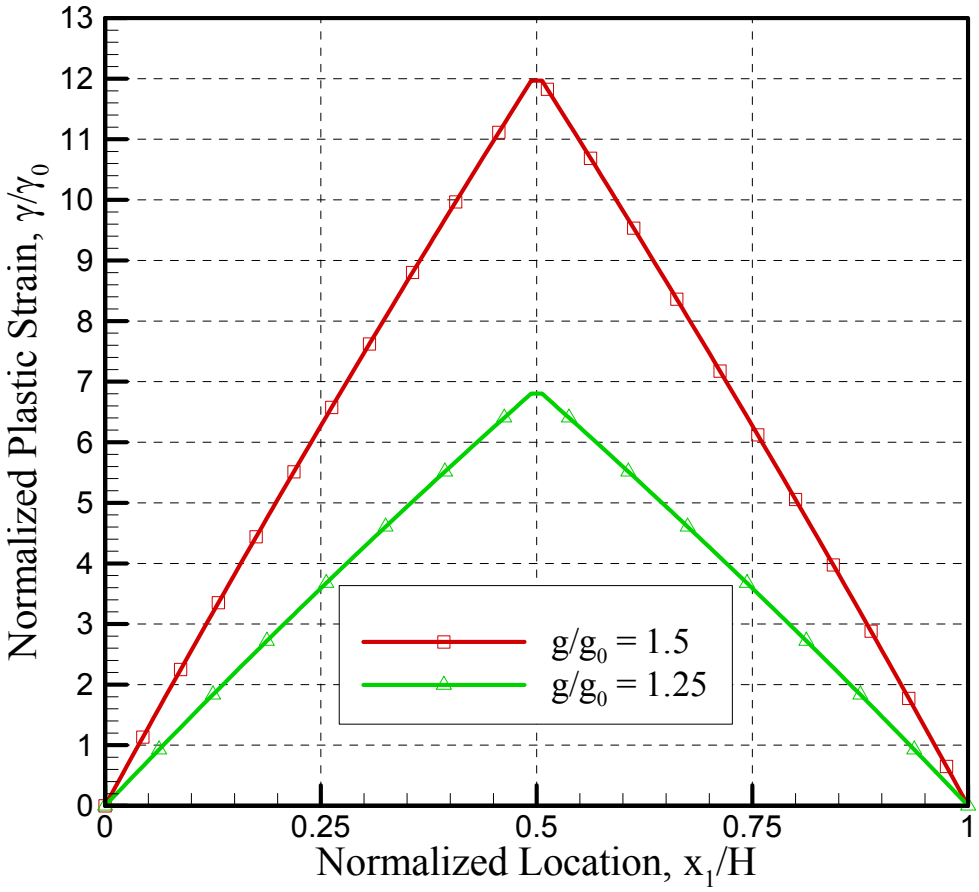

16(c)

Figure 16. a) Result corresponding to Figure 4 with hardening according to Eqn. (30); b) Result corresponding to Figure 10(b) with hardening according to Eqn. (30); c) Plastic strain profiles for initially upward parabolic distribution with hardening according to Eqn. (31) and no b.c.s applied.